A new method to predict the aggregate roughness of vegetation patterns on floodplains

Marloes B.A. ter Haar

September 2010

UNIVERSITY OF TWENTE.

A new method to predict the aggregate roughness of vegetation patterns on floodplains

September 2010

Master Thesis of:

M.B.A. ter Haar
Water Engineering & Management
University of Twente

Supervisors:

Dr. Ir. J.S. Ribberink
Water Engineering & Management
University of Twente

Dr. F. Huthoff
Water Engineering & Management
University of Twente

UNIVERSITY OF TWENTE.

SUMMARY

Nowadays rivers are given more room in order to lower the water levels in situations with high discharges. These spaces, called floodplains, are not all year covered with water and thus vegetation will grow on these floodplains. The variety of vegetation is large and different types of vegetation occur on one floodplain. In protecting the land against a possible flood hydraulic model computations play an important role. To be able to do this in an accurate way the characteristics of the river have to be implemented, which also includes the vegetation on a floodplain. This vegetation is modeled as a resistance to the flow.

Due to computational limitations not all small details that describe the river characteristics can be taken into account in the model, for example the roughness patterns. Therefore weighting methods are used to convert multiple roughness values in one cell to one aggregate roughness value that covers the variation in roughness. Currently, the WA-method is the weighting method that is used in the model WAQUA when more than one roughness value is implemented in one grid cell. This method is based on a small number of WAQUA calculations with different roughness patterns. This method predicts an aggregate value independent of the pattern layout and is therefore not always very accurate in predicting the aggregate roughness. The aim of this research is to investigate whether it is possible to create an improved method that takes pattern characteristics into account.

A large series of model calculations with the two dimensional model program WAQUA are carried out to investigate which flow and roughness pattern parameters influence the aggregate roughness of the pattern. WAQUA is a two dimensional model program used for simulation of water movement and transport processes in shallow water and it is based on a vertically averaged approach of the flow field. Different situations are used in the model calculations where the pattern layout, water depth and grid size are varied.

The vegetation pattern layout can be subdivided into parallel oriented patterns, serial oriented and a pattern with multiple square patches (2, 4 and 9) spread over the area. These patterns can be distinguished from each other by the streamlining of the pattern. A parallel pattern has a high streamlining in the flow, followed by the patterns with patches and a serial pattern has a very low streamlining. Furthermore different coverings of rough vegetation on the area are used in the investigation.

The results of these model runs are the aggregate Chézy values that represent the overall flow field. It turns out that the relative serial or parallel direction has a large influence on the aggregate roughness. This can be explained by the existence of flow adaptation processes due to the smooth to rough vegetation transitions. These processes can be divided into two parts: i) a mixing layer along smooth-rough transitions parallel to the flow and ii) flow adaptation behind a rough patch due to transitions perpendicular to the flow direction. These processes induce an additional roughness on the area, apart from the different roughness of the vegetation. The influences of these mixing layers and adaptation lengths can be expressed as a correction on the aggregate Chézy value. This correction is based on the geometrical lay out of the vegetation pattern.

The aggregate roughness resulting from a complete serial pattern can already be adequately predicted by the complete serial function and thus does not need be included in the determination of the new prediction model.

In order to be able to determine a new prediction method the relations that were found in the results of the model calculations between parameters and aggregate Chézy values are used. The basic principle of the new prediction model is that the parallel function gives an over prediction of the aggregate Chézy value for all pattern types. This already existing parallel function calculates the aggregate Chézy value for situations where the smooth and rough vegetations are parallel oriented in flow direction over the whole area. There is thus an additional roughness that needs to be incorporated in order to reduce the aggregate Chézy value. It is assumed that the mixing layer and the adaptation of the flow are responsible for this additional roughness. These two flow adaptation processes can be expressed as a surface ratio relative to the total area and are the important parameters in the new prediction method.

First the parallel patterns are used in order to incorporate the influence of the mixing layers on the area. These pattern types are used for this because in this situation no adaptation of the flow is present and thus the only factor inducing the additional roughness is the mixing layer. When the number of mixing layers is known the additional roughness induced by the mixing layer can be calculated. Next, the additional roughness induced by the adaptation of the flow is determined in the same manner, but this time the vegetation pattern with two patches serial directed was used. This length however is dependent on the width of the rough patch and will thus vary per patch size.

The additional roughness is thus made up of two contributions: i) the influence of the mixing layer, which is expressed as the ratio between the total mixing layer width and the width of the rough vegetation area and ii) the ratio between the free space behind a rough patch and the length of the rough patch. If the adaptation length fits between patches then the adaptation length is used in terms of the free space.

It turns out that this new prediction model is better capable of predicting the aggregate Chézy values than the WA-method that is currently used. The percentage of the predicted Chézy values that has less deviation from the measured values is 97.7 percent, against 25.6 percent of the WA-method predictions. The new model is validated using different patterns and eddy viscosity values than were used to deduce the model and it turns out that the prediction of the aggregate Chézy values for these situations is also very accurate. The new model needs to have small changes when situations with a different roughness ratio between the smooth and rough vegetation is implemented.

PREFACE

After finishing the bachelor Civil Engineering and Management at the University of Twente, I decided to start with the master course Water Engineering and Management. This thesis forms the completion of my master course at the University of Twente. My research describes a derivation of a new method to predict the aggregate roughness of vegetation patterns on floodplains.

Finishing this thesis would not be possible without the help of my supervisors. Therefore I would like to thank Jan Ribberink and Freek Huthoff for their help and time. During our meetings they gave me constructive feedback and suggestions. Also I would like to thank Jan and Freek for always having time to help me out with my problems.

I also thank my roommates of the graduation room and the employees of the WEM department for the social activities and lunches which were a welcome break from all the hard work. I enjoyed spending my time in the graduation room and the group activities we had, especially the barbeque and the hot potting.

Further I would like to thank my family, friends and especially Bob for all the evening and weekend breaks which were a welcome variation from work.

Marloes ter Haar
Enschede, September 2010

CONTENTS

LIST OF FIGURES AND TABLES

LIST OF FIGURES

LIST OF TABLES

1 INTRODUCTION

In this chapter an introduction will be given of the problem that is considered in this study. First the background of the study will be shortly explained, in order to give insight in the importance of modeling the characteristics of a river properly. Secondly a short description is given of a floodplain followed by the way in which vegetation on a floodplain is modeled at this moment. After that the problem analysis states what the problems are that are faced when it comes to modeling vegetation. Based on this problem the objective and the research questions are defined and based on these research questions the approach of the study is given. In the final section the outline of the report is presented.

1.1 BACKGROUND

In the last decades the economic growth and the development of urban communities in the Netherlands has resulted in more pressure on free space. To obtain more land for building activities the width of the riverbed has been restricted in order to fulfil the needs. One way to do this is by canalization, by which the river is made more straight and is bounded by dikes. These dikes have been raised during the years in order to keep the area behind the dikes safe against a possible flood. This may result in larger damages after a flood because the water level is higher and the economic value behind the dikes has increased.

Due to climate change the discharge of the rivers will further increase in the future. An option to protect the area within the dikes is to raise the dikes even further, however from a technical point of view this is not an option. Therefore another course has been adopted in the Netherlands: 'Room for the river'. The trend in this course is to give the river more room to flow in, in order to lower the water levels (Projectorganisatie Ruimte voor de Rivier, 2007).

Different measures can be taken in giving more room to the river. Some of the measures are: lowering the groins, lowering the summer bed, removing obstacles in the floodplain, lowering of the floodplains and widening the floodplain. A great deal of the measures incorporates building or adapting a floodplain, which has to lower the water level. In protecting against a possible flood hydraulic model computations play an important role. The results of the computations are crucial for acceptance or rejection of developments in the river system (Van Velzen et al., 2003). It is thus important to describe the flow over a floodplain accurately in order to design a measure that will lower the water level sufficiently. This modeling can be done with a 2D river model called WAQUA that is used in The Netherlands (Vollebregt et al., 2003 and for some examples see Svašek Hydraulics, 2010).

1.2 FLOODPLAIN

A floodplain is the area between the winter dike and the summer dike next to a river. It is the space that is reserved for the river to be able to cope with peak discharges. In case of a high water level in the river the main channel cannot hold all the water and it will start to flow over the floodplain. The floodplain then becomes a part of the river in order to be able to discharge the water. In figure 1 a cross section of a river with a floodplain is given. When there is no water on the floodplain vegetation will grow on it. The roughness of the vegetation determines the flow structure on the floodplain and its conveyance capacity and thus has an influence on the water level during a high discharge.

Furthermore, by temporary storing more water, the floodplain lowers the water level downstream of that location.

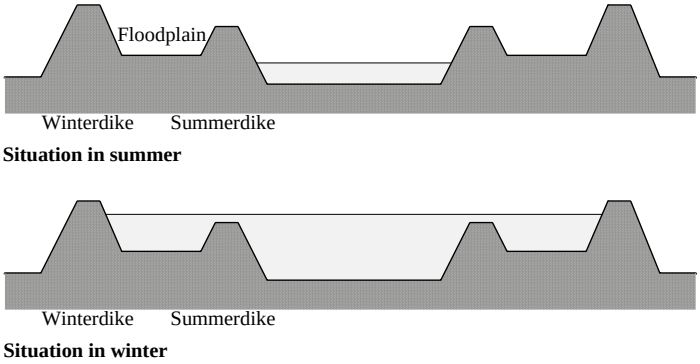

Figure 1: Cross section of a river with a floodplain (top: low discharge; bottom: high discharge).

To get insight in the types of vegetation on a floodplain, maps of ecotypes are used. These charts present the vegetation structure and are obtained from aerial photographs. From these photographs the structure of the different vegetation types are visual distinguished. When interpreting a photo it is not possible to account for every detail on the floodplain. This means that small groups of trees or bushes will not be taken into account in the analysis (Rijkswaterstaat, 2010a & Van Velzen et al., 2003). In figure 2 a part of an ecotype map retrieved from Rijkwaterstaat (2010b) is included from the Waal at Nijmegen and Beuningen in the Netherlands. The land that is shown next to the river represents floodplains. This map shows that different types of vegetation on a floodplain are available for input for model calculations.

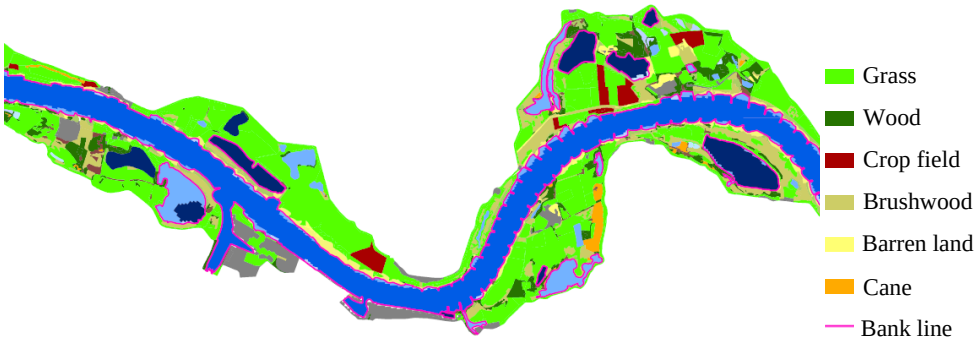

Figure 2: Zoom in of an ecotype map of the river Waal at Nijmegen and Beuningen (Rijkswaterstaat, 2010b).

1.3 MODELING VEGETATION

When a river is modeled the important aspects that can influence the flow in that river needs to be incorporated in the model in order to produce results that are accurate and meaningful. This includes the floodplain, which means that the vegetation on the floodplain needs to be represented in the model input. This vegetation is implemented as a resistance factor in the flow. This resistance is dependent on the height, frontal area, a resistance coefficient and the roughness of the bed (Van Velzen et al., 2003). Different vegetation types will thus induce a different resistance to the flow. Because a variety of vegetation is present on a floodplain, patches with different resistances to the flow are present. This

means that when the floodplain is modeled these varying resistances must be incorporated in the model description.

The resistance due to vegetation is implemented by a roughness parameter. Because it is not possible to account for every detail, grid cells with a certain size are defined. The input in one grid cell needs to be uniform, and thus a roughness variation within the grid cell cannot be represented, and one roughness value is given instead of the pattern. This process of replacing a pattern of roughness values by one roughness value will exclude a degree of accuracy, which is also influenced by the size of the grid cells that is chosen in the model, because the larger the grid cell the higher the chance that there are more vegetation types captured in one cell.

SOBEK and WAQUA are two different flow models that are used in The Netherlands. SOBEK is one dimensional and WAQUA is two dimensional. In SOBEK large cells are used that can represent areas of hundreds of square meters and in WAQUA grid sizes of several square decameters are used (Gao, 2004, RWS-Waterdienst & Deltares 2009a, 2009b) The degree of accuracy that is lost by excluding a roughness pattern is thus also different per flow model that can be used. In order to reduce the inaccuracy, weighting methods weight the pattern of roughness values to one value. In this way the effect of a pattern is captured in one value. In the following sub paragraphs two methods that are designed to do this are explained, first the weighted k summation method and after that the weighted average method which is used in the model WAQUA at this moment.

1.3.1 WEIGHTED K SUMMATION METHOD

A method to calculate an aggregate Chézy value is presented in Van Velzen & Klaassen (1999). At that time the method 'weighted k summation method' (from now on referred to as WKS-method) was used. This method is a variation to the suggested method grid averaging by Van Urk (1983, according to Van Velzen & Klaassen (1999)), in which is recommended to sum the Nikuradse k-values up by area division. It is tried to develop a method to describe the vegetation patterns. For that a distinction is made between serial and parallel flow direction, see figure 3. Van Urk (1983, according to Van Velzen & Klaassen (1999)) concluded that there are large differences between these two types of flow directions. However, it was not possible to point out how the flow resistance due to a patch of trees would be in proportion of the parallel or serial flow situation.

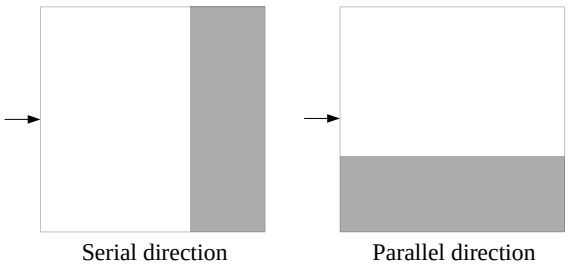

Figure 3: Parallel and serial flow direction (Van Velzen & Klaassen, 1999)

The WKS-method in formula:

$$k_t = k_g(1 - x) + k_b x \qquad [1.1]$$

With:

k_t = Representative k-value of the different vegetation types [m]

k_g = Nikuradse value of the basis vegetation [m]

k_b = Nikuradse value of group(s) of trees/bushes [m]

x = Part of the area covered by trees/bushes [-]

The Chézy value belonging to a certain Nikuradse k-value can be calculated using the following formula (Ribberink & Hulscher, 2008):

$$C = \frac{\sqrt{g}}{\kappa} \ln\left(\frac{12h}{k_n}\right) \quad [1.2]$$

With:

C = Chézy value [$m^{1/2}/s$]

g = Gravitational acceleration [m/s^2]

κ = Von Karman constant (0.41) [-]

h = Water depth [m]

k_n = Nikuradse value [m]

This WKS-method has two disadvantages; first of all it is never been tested and secondly the influence of grouping of vegetation and the direction to the flow of the vegetation is not taken into account. Van Velzen & Klaassen (1999) tested this method with use of the model program WAQUA and tried to refine this method in order to eliminate these two disadvantages. Three different formulas are deduced, one for parallel flow, one for more spread vegetation and one for one group of trees, these formulas can be found in Appendix I. In the study different patterns were investigated which are characterized by grouping and frontal shape; an aerial view can be found in Appendix II.

The patches in these patterns are covered with rough vegetation and cover approximately twenty percent of the total area. The vegetation roughness of bushes and trees were included as Chézy roughness values of respectively 4.8 $m^{1/2}/s$ and 42.9 $m^{1/2}/s$ and the water depth was kept as constant as possible at 5 m. The total discharge was the result of the model runs and with this discharge the aggregate Chézy value was calculated using the inverse Chézy formula:

$$C_t = \frac{Q_{waqua}}{hB\sqrt{h\frac{\Delta h}{L}}} \quad [1.3]$$

With:

Q_{waqua} = Discharge [m^3/s]

h = Average water depth (5m) [m]

B = Width [m]

Δh = Difference in height due to the slope [m]

L = Length area [m]

The conclusion was that the formula for spread trees/bushes suffices (formula b in Appendix I). But if the trees/bushes are placed in groups (patches) than the formulation for spread vegetation is unfavorable. The smaller the patches, the larger the relative energy dissipation until eventually the limit of energy dissipation of spread vegetation is reached. The dependency of the size of the patches and the number of patches was hard to formulate. Therefore, for vegetation in more groups, the old WKS-method was advised to use. In Appendix III the figures are included showing the Chézy values plotted together with the WKS-method. The prediction of the WKS-method is based on the Nikuradse values and the covering of rough vegetation and smooth vegetation, which gives in this case per

covering an equal prediction. The difference in Chézy value between the WKS-line and the result is the deviation of the prediction with the WKS-method for that particular pattern.

1.3.2 WEIGHTED AVERAGE METHOD

In Van Velzen et al. (2002) another method is given instead of the WKS-method because with certain vegetation combinations the WKS-method leads to an overestimation of the roughness. The newly proposed method, the weighted average method (from now on referred to as the WA-method), is based on the individual formulas to calculate the Chézy roughness for a serial and a parallel pattern see formulas 1.4 and 1.5 (Ministry of Transport, Public Works and Water Management, 2008). The derivation of these formulas can be found in Appendix IV.

$$C_p = \sum_i x_i C_{ri} \qquad [1.4]$$

$$C_s = \frac{1}{\sqrt{\sum_i \frac{x_i}{C_{ri}^2}}} \qquad [1.5]$$

With:

X_i	= Area fraction roughness type i	[-]
C_{ri}	= Chézy value roughness type i	[$m^{1/2}/s$]
C_p	= Chézy value for parallel pattern	[$m^{1/2}/s$]
C_s	= Chézy value for serial pattern	[$m^{1/2}/s$]

The WA-method used in the model WAQUA when a pattern needs to be converted to a single Chézy value is combined out of these parallel and serial approaches:

$$C_{cr} = \varphi C_s + (1 - \varphi) C_p \qquad [1.6]$$

With:

C_{rc}	= Average Chézy coefficient	[$m^{1/2}/s$]
C_s	= Chézy coefficient with serial pattern	[$m^{1/2}/s$]
C_p	= Chézy coefficient with parallel pattern	[$m^{1/2}/s$]
φ	= Weighting factor	[-]

In order to obtain a value for φ, Van Velzen et al. (2002) plotted the line obtained with equation 1.6 in such a way that it went on average as good as possible through the different patterns (1, 2, 3 and 4 as used in Van Velzen & Klaassen, 1999). It turned out that this factor was 0.6. This can be seen in Appendix III where the figures are included. It is also clear from these figures that with a small percentage woods or bushes the Chézy value changes a lot, the gradient is strong, and with a high coverage of rougher vegetation the gradient gets lower.

1.4 PROBLEM ANALYSIS

The WA-method of defining the Chézy value for a vegetation pattern on the floodplain is used in the model WAQUA when more than one Chézy value per grid cell is given (Ministry of Transport, Public Works and Water Management, 2008). This model is used as an advisory tool in order to foresee the effects of certain measures in the water system in the Netherlands (Vollebregt et al., 2002). A wrongly

defined roughness value on the floodplain will result in inaccurate flow properties, such as water level and flow velocity. When a measure has to be designed in order to agree with a certain water level that occurs with a specific return period, these inaccurate results will lead to a measure that is too safe or not safe enough according to the safety requirements.

Van Velzen et al. (2002) stated that the value of 0.6 in the WA-method can only be used when there is a possibility for the flow to redistribute. This means that the flow will follow the route with the lowest resistance and will flow over the areas with a high Chézy roughness value. But no limits are given to point out what is a redistribution of the flow and what not, the range of applicability is thus not very clear. Taking a value of 0.6 for φ means that it is always assumed that sixty percent of the vegetation is oriented serial to the flow direction and forty percent parallel. This is of course not always the case as for example in the patterns that were used in the assessment.

The WA-method is based on a few model runs. In these runs no variation was made in water depth, grid size and vegetation pattern which are all factors that vary from one floodplain to another. These different parameters might have an effect on the combined roughness value in WAQUA because every floodplain is different and the latest developments in airborne laser scanning and spectral remote sensing lead to the development of more precise vegetation maps (Straatsma & Baptist, 2008). When the same grid cell sizes are used as now, but with more precise input information, the WA-method will be used more often to calculate an aggregate roughness value.

Also, experiments revealed that the effective friction factor increases when roughness patterns are present (Van Prooijen, 2004 and Vermaas, 2008). Furthermore in the figures of Van Velzen et al. (2002), in Appendix III, it can be seen that not all the aggregate Chézy values resembling a roughness pattern lay perfectly on the line representing the WA-method, and thus do not correspond to the value that is calculated by the WA-method. A deviation from this WA-method thus means that it will under or overestimate the roughness value. This deviation will eventually lead to a modeled water level in WAQUA that is based on a wrong aggregated roughness value.

If flow over a floodplain is modeled not all the details can be taken into account because of computational limits or the information is not available and if it is available the inclusion of them takes too much time and effort. It is thus necessary to model a floodplain as good as possible with the least input data. A weighing method or some kind of model that can give a good representation of the vegetation pattern is thus needed.

The current problem is that the WA-method has not been properly tested and that no sufficient amount of variations in patterns and situations were used in order to deduce the method, which resulted in a method that predicts per covering percentage of rough vegetation the same aggregate roughness value, no matter of the layout of the pattern. This results in the fact that the incorporation of the WA-method in WAQUA may result in too large deviations between the actual aggregate roughness and the modeled roughness value.

1.5 RESEARCH OBJECTIVE AND QUESTIONS

The objective of this study is to get insight in what way patch parameters influence the aggregate roughness of a vegetation pattern and to deduce a method in predicting this aggregate roughness.

In order to reach the objective of the study the following question needs to be answered.

How can an improved model for floodplain roughness be developed which incorporates the influence of roughness pattern variation.

The next questions will help to answer the main question:

- How can the vegetation pattern be characterized in general parameters that control the aggregate roughness?
- How do the water depth and grid size of the model have an influence on the aggregate roughness obtained with the model WAQUA on a floodplain with a pattern of two vegetation types?
- What is the deviation of the aggregate roughness value obtained from WAQUA model runs with different patterns of roughness patches compared with the WA-method?
- Can an improved roughness prediction method be developed instead of the WA-method by taking into account additional control parameters?

1.6 APPROACH

To achieve the research objectives in paragraph 1.5 the following research approach is used.

- The first step is to define different patterns, where geometrical dimensions are considered as characterizations for the vegetation pattern.
- When these dimensions are defined the model runs can be made with WAQUA in which the variables water depth and grid size are varied in order to investigate the influence of these variables on the aggregate roughness.
- If the results of the model runs are known, an analysis of the aggregate roughness values is made. These values will be compared with the WA-method and ‘serial’ and ‘parallel’ theories and the results of the different patterns are compared with each other in order to find out what the influence of the geometrical dimensions of the pattern is on the aggregate roughness value.
- Finally it is investigated how a new weighting method can be defined in order to predict the aggregate roughness when multiple vegetation types are present on an area.

The approach discussed above is visualized in the research model in figure 4.

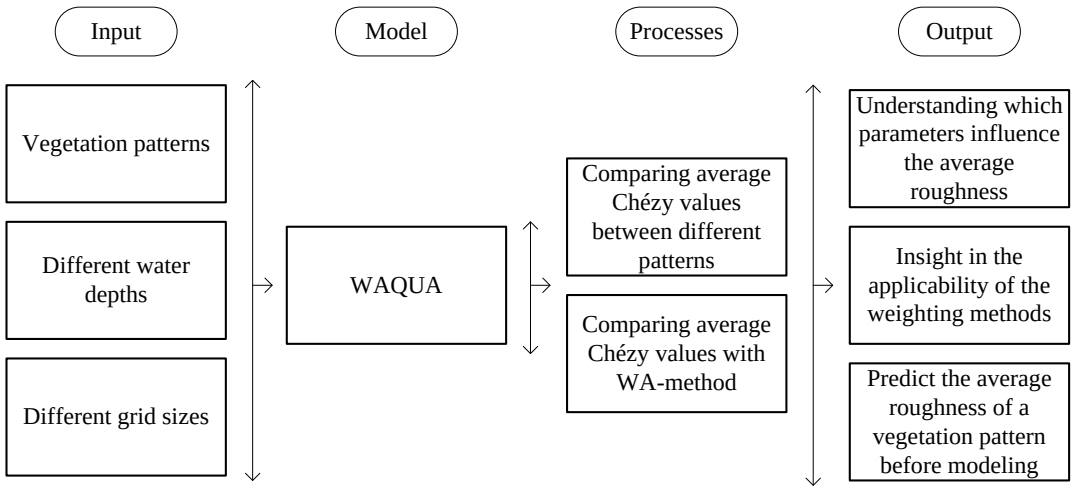

Figure 4: Research model

1.7 OUTLINE OF THE REPORT

In chapter 2 the important aspects for this study of the two dimensional model program WAQUA are presented. Chapter 3 contains the explanation of the flow adaptation processes that take place when there is a smooth to rough transition in bottom roughness. Also the special case of a complete serial pattern, where the total width of the area is covered with rough vegetation, will be shortly explained. After that, in chapter 4, the input description of the model calculations are given and the results of the calculations are presented. The derivation of a new prediction method is given in chapter 5, which is based on the results of the calculations. Chapter 6 gives the discussion and finally, in chapter 7, the conclusions and recommendations of this study are presented.

2 SHALLOW WATER FLOW MODELING

The model runs that are performed for this study are executed with WAQUA which is a program part of SIMONA which is provided by Rijkswaterstaat. Not all the features of WAQUA will be explained here, only the features that are important for this study. For a full description see Ministry of Transport, Public Works and Water Management (2008) and Ministry of Transport, Public Works and Water Management (2009b).

2.1 GENERAL

The two-dimensional model program WAQUA is used for simulation of water movement and transport processes in shallow water. It is based in a vertically averaged (two dimensional) approach of the flow field. The system can simulate hydrodynamics in geographical areas which are not rectangular, and bounded by any combination of closed boundaries (land) and open boundaries (b of Transport, Public Works and Water Management, 2008). The development started with the work of Leendertse, but the current methods are developed by Stelling in 1983. The model is for example used to schematize the rivers Meuse, Rhine and IJssel for computing the water levels in exceptional circumstances in order to decide on the required height of dikes to reduce the risk of flooding to an acceptable level (Vollebregt et al., 2002).

Rivers with their floodplains are typical examples of shallow water. Flood waves in rivers are often very slowly varying (duration of several days). The propagation speed of flood waves is small, of the same order as the flow velocity. This can be explained by the fact that bottom friction is a dominant effect in this case (Vreugdenhil, 1994).

2.2 SHALLOW WATER EQUATIONS

As discussed above WAQUA is used in flows where the characteristic horizontal length scales (dimensions of the flow domain and wavelength) are much larger than the vertical length scale (water depth). The flows are boundary layer types of flow. Therefore the motion of a fluid particle is mainly horizontal and the accelerations in vertical direction are neglected with respect to the gravity. Thus it is justifiable to neglect the vertical acceleration and advection. Also the vertical component of the Coriolis force and the stress components in the vertical direction may be neglected.

The shallow water equations that are used with a rectangular grid, excluding Coriolis and wind friction, are as follows (Praagman, 2005):

$$\frac{\partial u}{\partial t} + u\frac{\partial u}{\partial x} + v\frac{\partial u}{\partial y} + g\frac{\partial \zeta}{\partial x} + gu\frac{\sqrt{u^2+v^2}}{C^2(h+\zeta)} = \varepsilon\left(\frac{\partial^2 u}{\partial x^2} + \frac{\partial^2 u}{\partial y^2}\right) \quad [2.1]$$

$$\frac{\partial v}{\partial t} + u\frac{\partial v}{\partial x} + v\frac{\partial v}{\partial y} + g\frac{\partial \zeta}{\partial x} + gv\frac{\sqrt{u^2+v^2}}{C^2(h+\zeta)} = \varepsilon\left(\frac{\partial^2 v}{\partial x^2} + \frac{\partial^2 v}{\partial y^2}\right) \quad [2.2]$$

$$\frac{\partial \zeta}{\partial t} + \frac{\partial}{\partial x}(Hu) + \frac{\partial}{\partial v}(Hv) = 0 \quad [2.3]$$

With:

u,v	= Components of depth mean current	[m/s]
ζ	= Water elevation above plane of reference (see figure 4)	[m]
h	= Water depth below the plane of reference (see figure 4)	[m]
H	= $h + \zeta$	[m]
g	= Acceleration due to gravity	[m/s^2]
C	= Coefficient of Chézy to model bottom	[$m^{1/2}/s$]
ε	= Eddy viscosity coefficient	[m^2/s]

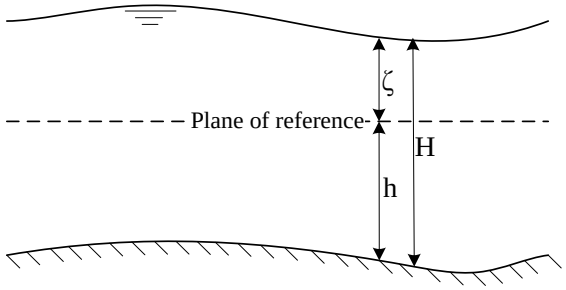

Figure 5: Layer of water is water depth plus water elevation

2.3 GRID

The computational grid that is used in WAQUA is illustrated in figure 6. A grid is laid on the rectangular area, where the square grid space size in meters is chosen, and the number of grid spaces in two dimensions, Nmax and Mmax. Four basic physical properties pertain in each grid space: water level, depth, u-component of velocity and v-component of velocity. During the simulation different time integrals are computed using an ADI staggered time integration method over two half time steps, so not all primary data is available at the same time. At the first half time step the u-velocities and resultant water levels are calculated and also separate v-velocities (explicit). At the second half time step the v-velocities and resultant water levels are calculated together with the separate u-velocities (explicit).

The basis of the WAQUA system is the staggered grid. This implies that the modeling system can be seen as a large number of linked, column shaped, volumes of water. The corners of these volumes are the depth points of the grid. Each volume of water has four sides through which water may flow in or out of the volume (Ministry of Transport, Public Works and Water Management, 2008).

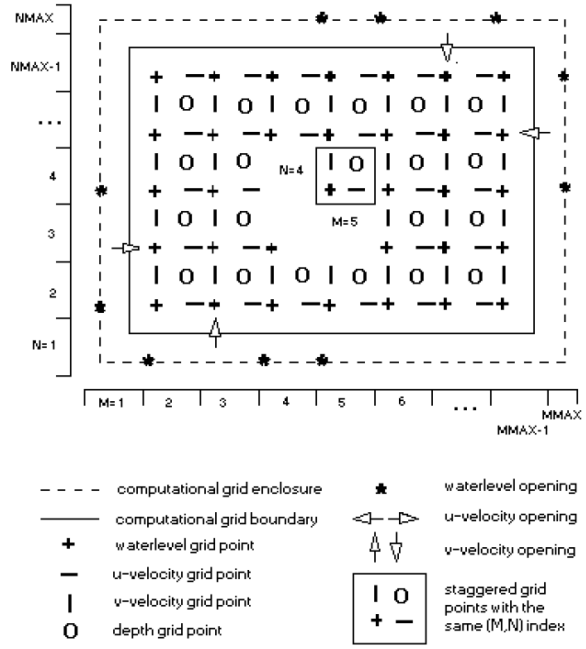

Figure 6: Default computational grid with arbitrary openings

2.4 BOUNDARIES

At the boundaries of the area information about these boundaries are needed. Two types of boundaries can be distinguished: closed and open boundaries. Closed boundaries are mostly locations that are bounded by land. Open boundaries are boundaries where water is bounded by water.

Open boundaries where river data are given to drive the model are needed. In the case of this study water level boundaries are given in which the water levels are given at the beginning and at the end of the model. In general, the open boundaries feed into the computational grid from just outside. This also implies that the ends of an open boundary do not extend beyond the grid.

2.5 EDDY VISCOSITY

In Uittenbogaard et al. (2005) a description of the eddy viscosity coefficient in WAQUA is given. It says that next to the friction at the surface of the water and at the bottom extra friction tensions are implemented due to the Reynolds averaging. These extra tensions are the Reynolds stress that takes into account the turbulent effects. WAQUA uses the eddy viscosity concept in order to solve this. This concept describes the Reynolds stresses as the product of the flow dependent eddy viscosity coefficient and the average gradient in the flow velocity. The viscosity coefficient is applied to bring, for example, the turbulent shear stresses into account. This means that with the implementation of a different eddy viscosity coefficient, the turbulent shear stresses can be influenced.

3 FLOW ADJUSTMENT PROCESSES

As already discussed in chapter 1, on a floodplain a variety of vegetation is present. This variation creates patches of various vegetation types. When there are patches of rougher vegetation present on an area, there will be transitions in flow velocities, because the water will flow faster above smooth vegetation than above rough vegetation due to the induced resistance. In order to comply with these differences the flow has to adjust itself. These adjustments give rise to processes in the flow around the smooth-rough transitions. These processes induce an additional roughness on the area, on top of the different roughness values of the vegetation. These adjustment processes are handled in this chapter. The adjustments are separated in three parts; i) a mixing layer that is located at the transition parallel to the flow direction, ii) an adaptation length on the lee side of a transition perpendicular to the flow direction and iii) a special situation where it is not possible for the flow to redirect around the rough vegetation, referred to as serial impact. In this chapter these three processes are explained and it is tried to predict the geometrical dimensions of them with use of the model WAQUA.

3.1 MIXING LAYER

White and Nepf (according to Zong and Nepf, 2010) described the flow structure and exchange at the interface between parallel regions of emergent vegetation in an open-channel. The drag discontinuity at this interface creates a shear layer that in turn generates large coherent vortices. This is also what happens at the interface of smooth and rough vegetation which is called the mixing layer. A larger part of this mixing layer lies above the smooth side than above the rough side (Vermaas, 2008, Van Prooijen, 2004). Figure 7 shows the transition of the velocity from high above the smooth side, to low above the rough bottom and to high again above the smooth side. The mixing width, δ, is the property that influences the aggregate roughness on the area.

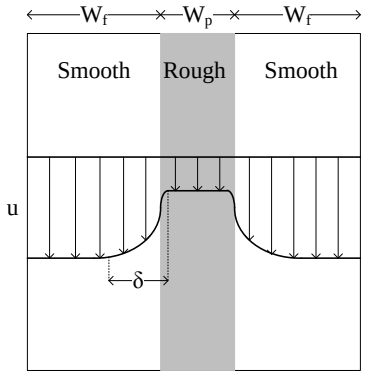

Figure 7: Representation of the mixing width when there is a transition from smooth to rough to smooth.

Van Prooijen (2004) executed experiments in order to gain a better understanding of the mixing layer. From the mean streamwise velocity data the characteristic properties of the downstream development of a shallow mixing layer were determined. These characteristics are: the decrease of the velocity difference, the non-linear widening of the mixing layer and the shift of the mixing layer to the low velocity side.

Also Vermaas (2008) executed laboratory experiments. The bottom consisted out of a hydraulically rough and smooth section in parallel direction of the flow. Measurements were done for five different depths and discharge settings. Due to the different roughness's between the sections, the flow decelerates above the rough side and accelerates above the smooth side. When the mixing layer is under development, the flow redistributes, water volume is transferred from the rough to the smooth side. In the developed part of the mixing layer, the bed shear stress above the rough side is higher than at the smooth side. This requires longitudinal momentum to be transported from the smooth to the rough side in order to maintain a mixing layer that is uniform in x-direction.

When a parallel pattern is implemented in WAQUA the mixing layer is constant along the length of the area and it is situated more to the smooth side. The other characteristics that were found with the experiments executed by Van Prooijen and Vermaas are not present in the results of WAQUA. This is because WAQUA is a depth averaged flow model that uses a constant eddy viscosity without modeling turbulence in detail. The eddy viscosity coefficient thus has a large influence on the mixing layer width.

Since all the model runs in this study will be executed with the WAQUA model, first the behaviour of the mixing layer will be shortly studied with some specific model runs. A parallel pattern type is used in order to determine the mixing width. The grid size is 20 m, slope $1 \cdot 10^{-4}$ and the total area 1000 by 1000 m. First the influence of the eddy viscosity coefficient will be studied followed by the water depth to increase the understanding of the important factors that influence the mixing layer in this study.

3.1.1 EDDY VISCOSITY

To understand what this eddy viscosity terms does model runs were executed where the eddy viscosity is varied. A parallel vegetation pattern is implemented with W_f of 700 m and W_p of 300 m which means a covering of thirty percent rough vegetation. The water depth at the beginning and end of the area is set at 5 m. In Table 1 the discharge and the aggregate Chézy values can be found.

Eddy viscosity [m^2/s]	0.5	5	10
Discharge [m^3/s]	3442	3319	3246
Chézy [$m^{1/2}/s$]	30.8	29.7	29.0

Table 1: results model runs with varying eddy viscosity

This table shows that if the eddy viscosity term is larger, the area discharges less water and the mean roughness of the area is thus larger. This can be explained with the wider mixing width with a larger eddy viscosity value. In Figure 8 the pattern that is used is shown on the top left and the other three figures show the flow velocity values. Blue indicates a low velocity and orange a high velocity. In the figures it can be seen that the transition from low to high becomes wider with a higher eddy viscosity. Changing this coefficient can thus have a large influence on the results.

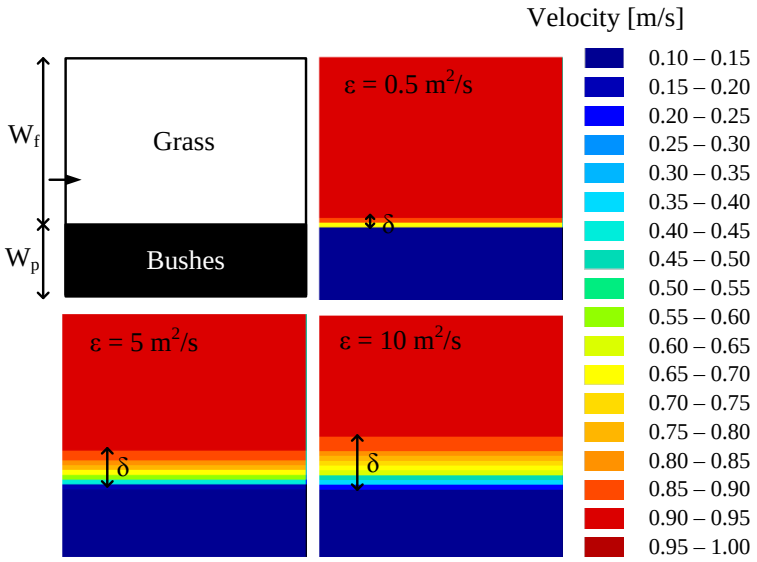

Figure 8: On the top left the parallel pattern is included. The other three figures are the flow velocities [m/s] for situations with an eddy viscosity of 0.5, 5 and 10 m^2/s.

In figure 9 the mixing width in meters is plotted against the eddy viscosity coefficient. The results are obtained from calculations similar as the situations shown in figure 8. These widths are determined from a parallel pattern with a water depth of 5 m where only the eddy viscosity has been varied; all the other parameters were kept constant. Plots with steps of 0.05 m/s in flow velocity are used to determine the mixing layer width which is assumed to be an accurate representation of the flow field.

The form of the relationship between the mixing layer width and the eddy viscosity coefficient, shown in figure 9, indicates that the mixing width and the eddy viscosity have the following dependence:

$$\delta \sim \sqrt{\varepsilon} \qquad [3.1]$$

It can thus be concluded that when the eddy viscosity coefficient is changed in the model WAQUA the mixing layer will vary in width and thus has an influence on the aggregate roughness.

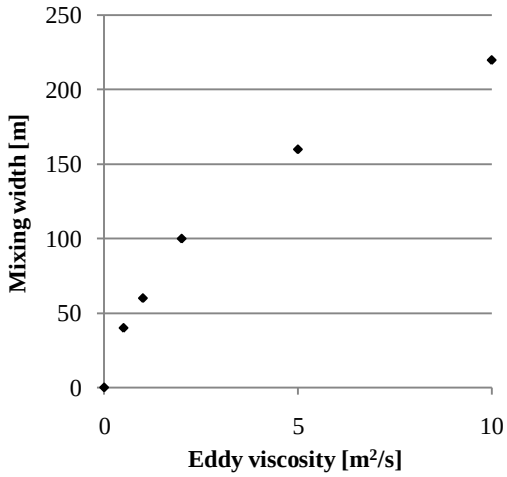

Figure 9: The mixing with plotted against the eddy viscosity value.

3.1.2 WATER DEPTH

Also different water depths are used to investigate what the influence is of this parameter; 3, 5 and 7 m (explanation of the choice of these water depths will be given in chapter 4). The same parallel pattern as in paragraph 3.1.1 was used to determine the influence of the eddy viscosity on the mixing layer.

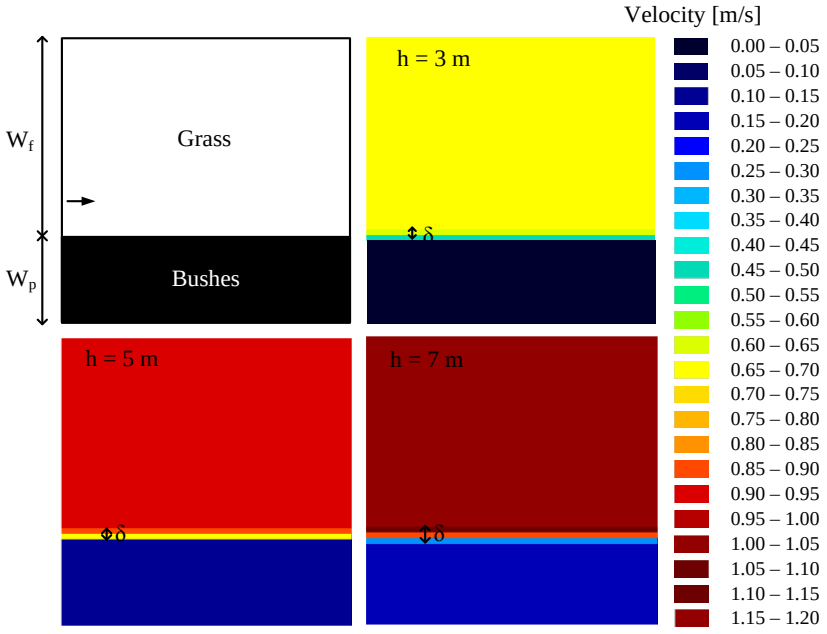

Figure 10: On the top left the parallel pattern is included. The other three figures are the flow velocities [m/s] for situations with water depths of 3, 5 and 7 m.

Because with a larger water depth a relatively smaller part of the water column is affected by the vegetation, the overall roughness will be smaller. This gives rise to different velocity differences between situations with another water depth. This is because the difference in flow velocity above the smooth and rough side increases with a larger water depth. For a water depth of 3 m the flow velocity of the smooth side is approximately 0.65 m/s and above the rough vegetation side 0.01 m/s which gives a difference of 0.64 m/s. With a water depth of 7 m the flow velocity above the smooth side is 1.2 m/s and above the rough side 0.2 m/s which gives a difference of 1 m/s which is larger than the difference in the 3 m situation.

In table 2 the mixing layer widths per water depth are given. When a different water depth is present in WAQUA the water depth will thus have an influence on the mixing layer width, although small compared to the influence of the eddy viscosity coefficient. This will be taken into account in this study.

	h = 3 m	h = 5 m	h = 7 m
Mixing layer width [m]	40	40	60

Table 2: Mixing layer widths belonging to a certain water depth

3.2 ADAPTATION LENGTH

After a rough patch, the flow will experience a smoother roughness and will thus gradually increase flow velocity. The distance that the flow needs to recover from the disturbance in the flow is the adaptation length. An indication of Sieben (2006) is that with a shallow water flow the length scale is more than 20 to 50 times the water depth. Taking a water depth of 5 m means that the length scale ranges from 100 till 250 m.

Labeur (1998) gives a description of how long the distance is that is needed for the flow to adapt to the new situation after a sand pit. This adaptation length is corrected for very wide sand pits, with the following formula:

$$\lambda' = 1/2 \frac{\beta B}{\sqrt{(\lambda^2 + \beta B)} - \lambda} \qquad [3.2]$$

With:

$$\lambda = \frac{C^2 h}{2g} \qquad [3.3]$$

λ	= Adaptation length	[m]
λ'	= Adapted adaptation length to width of the pit	[m]
β	= Equivalent width	[m]
B	= Width of the sand pit	[m]
h	= Water depth	[m]
C	= Chézy coefficient	[$m^{1/2}/s$]
g	= Acceleration due to gravity	[m/s^2]

The equivalent width value has not been deduced in Labeur (1998), but with an increasing value the adaptation length increases. It is shortly investigated whether this relation can also be used in the case of vegetation patches.

It is expected that the water depth has an influence on the adaptation length of the flow. Also the influence of the eddy viscosity value on the flow adaptation length is shortly investigated. With the use of some model runs with WAQUA the influence of these two parameters on the adaptation length is investigated. A large area, 4 by 4 km is used in order to capture the complete adaptation length. Square patches of rough vegetation (bushes) are implemented with varying patch size to investigate the influence of the width of the patch on the adaptation length. In the following paragraphs the influence of the parameters are investigated.

3.2.1 EDDY VISCOSITY

Situations with varying eddy viscosities are made with one square patch in order to investigate the influence of the eddy viscosity coefficient on the adaptation length of the flow at the lee side of the patch. The water depth is 5 m. Figure 11 shows a zoom in of the flow velocities around the patch for different eddy viscosities. The left top figure gives the pattern, with the black area indicating the rough vegetation. From this figure it can be concluded that the adaptation length behind a patch decreases in length with increasing eddy viscosity, but increases in width. This is because when the eddy viscosity

term is larger, the mixing layer is wider (see paragraph 3.1.1) and thus the width that is felt by the flow is larger with a higher eddy viscosity value.

The flow velocities above the patch are increasing with higher eddy viscosity values. The differences in flow velocities above the rough area and above the smooth area decrease with increasing eddy viscosity value. The adaptation of the flow thus needs a smaller length to adapt to the new flow situation above the smooth area; this can explain the minor decrease in adaptation length with increasing eddy viscosity coefficient.

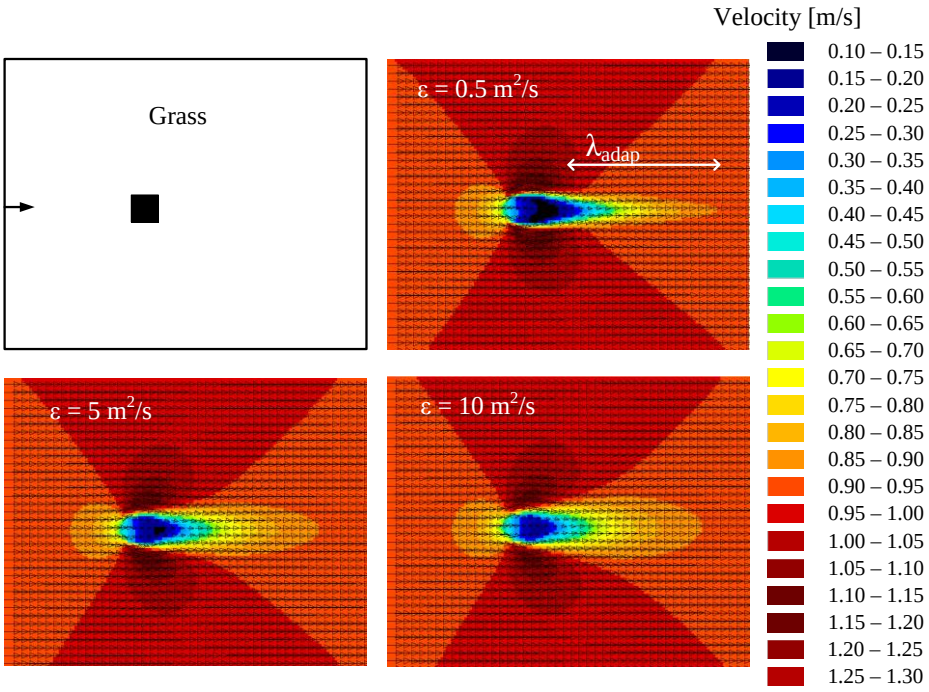

Figure 11: The top left figure gives a zoom in on the pattern. The other three figures show a zoom in of the area showing the flow velocities [m/s] for situations with an eddy viscosity of 0.5, 5 and 10 m^2/s.

The adaptation length is obtained from figures given in figure 11 with a velocity step of 0.05 m/s which is assumed to be a reasonable accurate representation. The length that is needed to reach half the flow velocity belonging to a smooth situation is assumed to be half of the total adaptation length. Obtaining the adaptation lengths for the different situations with varying eddy viscosity coefficients gives the relation shown in figure 12. This figure also shows the decreasing adaptation length with increasing eddy viscosity.

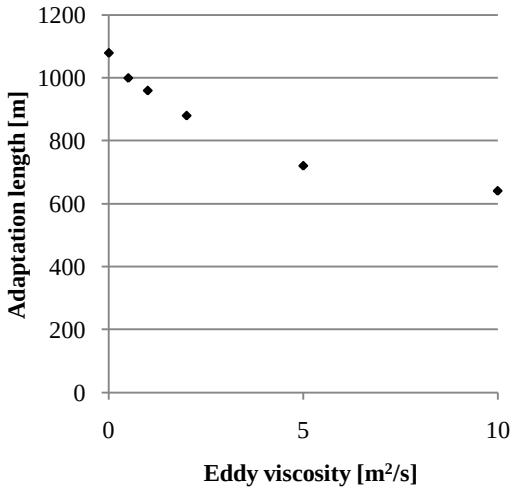

Figure 12: The adaptation length plotted against the eddy viscosity value.

Whether the influence of the eddy viscosity on the adaptation length will also affect the aggregate roughness of the area cannot be said for certain based on the above findings. Although the length decreases with an increasing eddy viscosity value the width increases and thus the total effect might be minor. Therefore the discharges of the total areas are given in table 3. This table shows that the discharges are almost equal and thus the influence of the eddy viscosity coefficient on the adaptation length will be neglected in this study.

Eddy viscosity coefficient [m^2/s]	0	0.5	1	2	5	10
Discharge [m^3/s]	18918	18919	18919	18916	18905	18886

Table 3: Results in discharges for model runs with one square patch and varying eddy viscosity coefficient.

3.2.2 WATER DEPTH AND WIDTH OF ROUGH VEGETATION

Model runs with different patch sizes were carried out in order to investigate the influence of the patch width on the adaptation length, the water depths are 3, 5 and 7 m. The length of the adaptation is determined by figures showing the flow velocity in steps of 0.05 m/s. When the flow velocity in the adaptation area was half of the flow velocity above the smooth area this length was taken as half the adaptation length. In figure 13 the total adaptation length is plotted against the width of the patch. The adaptation length increases with an increasing width of the patch and thus shows the same relationship that Labeur (1998) showed with formula 3.2 with an increasing value for β. When the size of the patch increases this automatically means that the covering of rough vegetation increases and the figures in Appendix III show that an increasing covering means an increase in roughness.

With an increasing water depth the adaptation length also increases with almost a doubling of length from 3 to 7 m water depth. This can also be explained by the difference in flow velocity that needs to be reached by the flow between the different water depths. The larger the difference in flow velocity the longer the distance the flow needs to adapt itself to the new conditions.

It can thus be concluded that the width of the patch and the water depth have an influence on the length of the adaptation of the flow behind a rough patch.

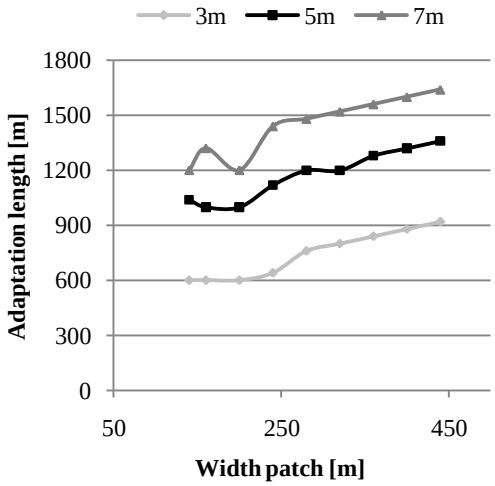

Figure 13: The results of the adaptation length plotted against the width of the rough patch for the different water depths.

It is tried using formula 3.2 and 3.3 to describe the results that are given in figure 13. It turns out that no acceptable representation for β can be obtained to represent the results in figure 13. Therefore a function will be set up to use in this study to calculate the adaptation length for varying water depth and patch size because these two parameters are of most influence on the length.

$$\lambda_{adap} = f(h, W_p) \qquad [3.4]$$

The fitted line should represent the results in figure 13 as good as possible. Because the increase in adaptation length per increase in patch width is almost equal for the three water depth situations the slope for the new function should be constant per water depth. The influence of the water depth can be expressed in the constant of the function. The equation of the line is:

$$\lambda_{adap} = \alpha h + \beta W_p \qquad [3.5]$$

With λ_{adap} the predicted adaptation length. The values for α and β are defined by finding a method such that (Davis, 2002):

$$\sum \left(\lambda_{adap} - \lambda_{adap,measured}\right)^2 = minimum \qquad [3.6]$$

The minimum value of formula 3.6 is found at values for αand βof respectively 171 and 0.97, filling this in formula 3.5 gives the function that is used in this study to calculate the adaptation length behind a rough patch:

$$\lambda_{adap} = 171h + 0.97W_p \qquad [3.7]$$

In figure 14 the results and the predicted values are plotted in one figure. The solid lines indicate the measured values and the dotted lines the predicted values. Equation 3.7 will be used in the remainder of this study if the adaptation length needs to be calculated.

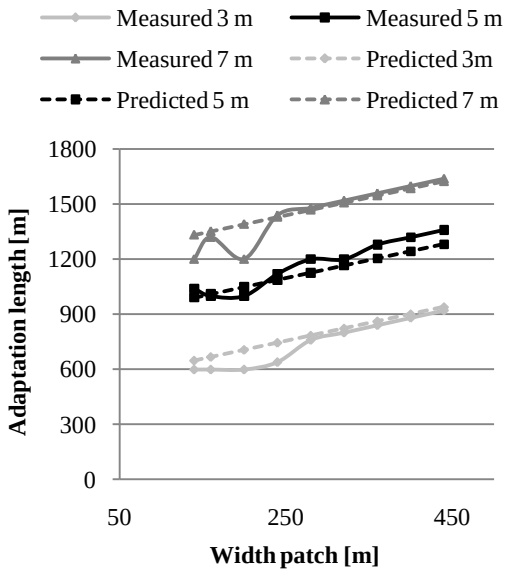

Figure 14: The measured (solid line) and the predicted (dotted line) adaptation lengths plotted against the patch width for different water depths.

3.3 SERIAL IMPACT

The above mentioned flow processes occur when the flow can follow a free pathway above the smooth vegetation. There is one situation in where this is not possible; when the vegetation covers the total width of the area. In this situation the flow on the total area is influenced by the rough vegetation and also no adjustment processes as discussed above are present.

Van Urk, according to Van Velzen & Klaassen (1999) already concluded that the difference between a complete serial and parallel orientation to the flow is large. The influence of backwater effects plays a role in this serial situation. These backwater effects arise because the water can flow freely until it reaches the complete strip of rough vegetation. At this point the flow velocity decreases and the water depth will increase. This effect happens not at once and thus a backwater curve will arise before the rough vegetation where the water depth slowly increases. After the rough strip the same process takes place but there the water depth will slowly decrease again. However during the model runs that will be carried out in this study the water depth will be kept as constant as possible, just like Van Velzen & Klaassen (1999) did. This will probably eliminate the backwater effects.

One model run is carried out in order to investigate how the water depth behaves over the area. One stripe of rough vegetation is implemented, with a covering of 30 percent of rough vegetation and a water depth of 5 m. The resulting water depths in flow direction are shown in figure 15 with the black line indicating the water depth over the area and the grey dotted lines the start and ending point of the rough vegetation. That the water depth is given as input at the beginning and end of the area is very clear in this figure, both are exactly 5 m. The variation in water depth when the water flows over the area is very small, the extremes differ 0.033 m. It can be concluded that the backwater effects are very small when the water depths are kept as constant as possible and this results in a situation where the flow velocities on the area are constant.

The serial impact in this study is thus that the total area is influenced by the strip of rough vegetation and this reduces the flow velocities, and thus also the discharge and aggregate roughness, remarkable.

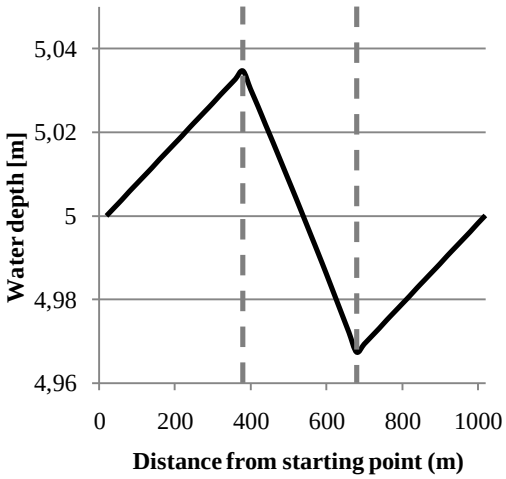

Figure 15: The water depths in flow direction, the grey dotted lines indicate the starting and end point of the rough vegetation.

4 WAQUA COMPUTATIONS

To be able to determine what parameters have an influence on the aggregate roughness on an area, different types of situations are used in the modeling calculations. In this chapter the model runs and their results are discussed. First, in paragraph 4.1, the manner in which the aggregate Chézy value can be calculated out of the model results is given. After that the input of the model WAQUA is discussed. Here also the parameters are defined of which it is expected to have an influence on the aggregate roughness. In paragraph 4.3 the model results are given, which are the aggregate Chézy values. These results can help in finding the influence of particular parameters on the aggregate roughness and will improve the understanding of the processes that take place.

4.1 DETERMINING AGGREGATE CHEZY VALUE

To calculate the aggregate Chézy value out of the results of the model runs, the total discharge is needed. At the end of the area the total q [m^2/s] is taken for all grid cells in that row. Multiplying this q by the size of the grid cells and adding them gives the total Q [m^3/s]. Because the water depth is kept as constant as possible, the aggregate Chézy value can easily be determined using the inverse Chézy formula:

$$C_t = \frac{Q_{waqua}}{hW_t\sqrt{h\frac{\Delta h}{L_t}}} \qquad [4.1]$$

With:

Q_{waqua}	= Discharge	[m^3/s]
h	= Average water depth	[m]
W_t	= Width total area	[m]
Δh	= Difference in water level due to the bed slope	[m]
L_t	= Length area total area	[m]

4.2 SET UP

The input for the model can be divided in two types, fixed and variable. The fixed model input is the input that is kept constant for all situations, for example the slope. The variable input exists out of the parameters that are varied in order to investigate the influence of these parameters on the aggregate roughness. An example of the variable input is the layout of the vegetation pattern. This paragraph will describe this input, starting with the fixed input.

4.2.1 FIXED INPUT DESCRIPTION

The area of investigation will have a squared shape and a slope in the bottom of $1 \cdot 10^{-4}$ which is fixed during the model run. For the water level this slope is implemented over the whole area as an initial condition. In order to find out how much water can be discharged with a certain water depth and bed

slope the water depth will be fixed at the same constant value at the beginning and end of the area during the run, the water depth above the rest of the area can vary. A cross section can be found in figure 16.

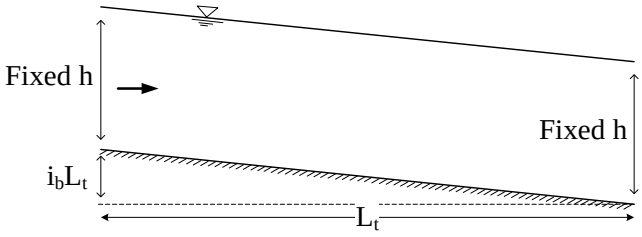

Figure 16: Cross section of the area

The size of the total area will be 1000 by 1000 m because this size was also used in the calculations done by Van Velzen & Klaassen (1999), and thus on which the WA-method is based. During the investigation two different types of vegetation are used to create the patterns of roughness types; grass and bushes. As input in WAQUA the Nikuradse k-values are given which is 0.25 m for grass and 33 m for bushes (Van Velzen & Klaassen, 1999). The Chézy value belonging to a certain Nikuradse k-value is in WAQUA calculated using the following formula (Van Rijn, 1990 according to Ministry of Transport, Public Works and Water Management (2008)):

$$C = 18 \log\left(max\left(\frac{12h}{k_n}, 1.0129\right)\right) \qquad [4.2]$$

With:

C	= Chézy coefficient	[$m^{1/2}/s$]
h	= Total water depth at the velocity point	[m]
k_n	= k-Nikuradse value	[m]
Max	= The 'maximum function'	

The maximum function is implemented to make sure that when the $12h/k_n$ is smaller than 1, which happens with really small water depths and high k-Nikuradse values, the Chézy value will not become negative.

Another parameter that must be given is the eddy viscosity coefficient. This coefficient is important for the mixing width between a smooth and rough bottom, as discussed in chapter 3. The default value given in Ministry of Transport, Public Works and Water Management (2009a) is 10 m^2/s and in RWS-Waterdienst & Deltares (2009) a value of 1 m^2/s is used. But in Boderie et al. (2005) and Uittenbogaard et al. (2005) it is mentioned that an eddy viscosity of 0.5 m^2/s will give the best results and this value is normally used in model calculations, therefore it is decided to implement this value instead of the default value.

4.2.2 PARAMETERS OF INVESTIGATION

In this sub paragraph the parameters are discussed that will be varied in the investigation. This is done in order to investigate whether these parameters have an influence on the aggregate roughness of the area. These parameters are defined based on factors that vary between different floodplains and on the increasing accuracy of input information that is available of floodplains. It will be explained why the parameters are taken into account and also to what extent these will be varied.

4.2.2.1 WATER DEPTH

Different water depths can occur on a floodplain, and thus when a floodplain is modeled water flows with different water depths have to be represented by the model. The prediction of the aggregate roughness, when a vegetation pattern is present in one grid cell, should be equally accurate in all times. Therefore the influence on the aggregate roughness of the water depth should be taken into account during the analysis.

Vegetation in the water will have a larger effect when the water depth is small than when the water depth is large. With the use formula 4.2 given in paragraph 4.2.1 figure 17 is made. This figure shows the Chézy values belonging per water depth for bushes (dotted line) and grass (solid line), which will be used to create the vegetation patterns.

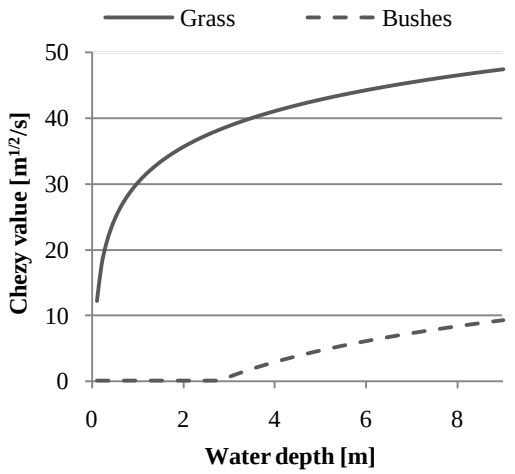

Figure 17: Chézy value for grass and bushes for varying water depths

This figure shows that how deeper the water is, the less rough the vegetation becomes. This is because relatively a smaller part of the water column is affected by the roughness on the bottom. It is also apparent that the Chézy value for bushes becomes really small with low water depths, almost approaching to zero, and is not changing until about 3 m water depth. Therefore taking water depths smaller than 3 m is not realistic and will not give extra insight in the processes taking place.

It can be concluded that different water depths will result in different Chézy roughness values on the area, therefore different water depths will be taken into account in order to investigate what the influence is on the aggregate roughness. Furthermore it is important to investigate whether it might be necessary to include the water depth in the prediction method of the aggregate roughness. Depths of 3, 5 and 7 m are taken because it is thought that these are realistic values.

4.2.2.2 GRID SIZE

New developments in airborne laser scanning may lead to more precise input information to represent the floodplain and might lead to the incorporation of a finer grid. A finer grid results in a more fine representation of a vegetation pattern, and thus also the flow adjustments (see chapter 3). Because in each grid cell the basic physical properties are calculated (see chapter 2) more information on the total area will be available when smaller grid sizes are implemented. It is thus desirable to investigate whether the grid size will have an influence on the flow processes and thus the aggregate roughness on the area.

The developments in airborne laser scanning will lead to more precise information and thus a smaller grid size than 20 m, which was also used in the experiments of Van Velzen & Klaassen (1999), will be used next to this size. Only the influence of the grid size must be investigated, all the other parameters must be kept constant, for example the sizes of the rough vegetation patches. This is a restriction in the choice of the smaller grid size, for example a grid size of 15 m is not possible because not the exact same vegetation patterns can be created as with a size of 20 m. Therefore it is chosen to use the largest value that complies with this restriction which is a grid size of 10 m, this is a factor four finer. This increase in fineness is thought to be a good representation of the influence of the grid size on the aggregate roughness. Moreover, because in every grid cell the basic physical properties are calculated, this grid size will give the least increase in calculation time.

4.2.2.3 PATTERN AND COVERING

Vegetation on a floodplain is almost never uniform but very heterogeneous. Different kinds of patterns can be made based on the flow adaptation processes that evolve. The mixing layer and the adaptation of the flow play a role, but a vegetation pattern can be situated such that the adaptation of the flow does not take place in the area of investigation. A special case is the complete serial pattern, where it is not possible for the flow to redirect around the rougher patches.

PARALLEL ORIENTED

When a pattern is complete parallel, there will not be an adaptation behind the patch of the flow, because there is no space left. Therefore the parallel pattern can be used in order to investigate what the influence is of the mixing layer. Splitting the rough strips into pieces, creating more strips, will induce more mixing layers on the area, and will thus probably make the area rougher. To investigate whether it is possible to predict the influence of the mixing layers on the aggregate roughness, parallel patterns will be modeled in where the number of strips is varied between 1, 2 and 3 pieces. Because the mixing layer widths are constant over the area (chapter 3) the free spaces between the lanes will be varied such that in one situation the mixing layers do not interact with each other (120 m) and in one situation they do (60 m). This is included because it can help in understanding the influence of the mixing layers more and because it needs to be investigated whether the number of mixing layers that are present influence the aggregate roughness substantially or not. In Appendix V figures are included that will clarify these pattern types; also the codes for the patterns are given in the left top corner.

MULTIPLE PATCHES

To introduce an adaptation of the flow behind the rough vegetation, patterns are created where the flow can redirect around the patches of rough vegetation. Patterns with a different number of squared patches can be made; one with two, four and nine patches. The more patches the more the pattern is spread out over the area. The pattern with two patches can be situated more parallel, behind each other in flow direction, and serial where the patches lay next to each other in flow direction. The patterns with four and nine patches are more squared in total. These lay out can also be distinguished by the amount of streamlining of the pattern. The more parallel the pattern is the better is the streamlining, the easier the flow can redistribute around the rougher area. The distances between the patches can also be varied. The outlay of these patterns is given in figure 18.

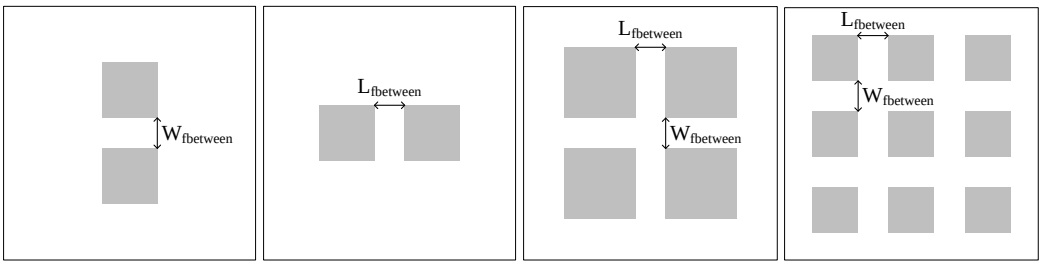

Figure 18: From left to right: two patches serial oriented; two patches parallel oriented; four patches; nine patches.

Just like the parallel patterns, the mixing layer is assumed to be constant over the total length of the rough patch and therefore two sizes of space between the patches transverse to the flow direction are used ($W_{fbetween}$); one where the mixing layers do not interact with each other and one where there is interaction. The adaptation of the flow behind the patches is very long and it is not possible to include this length in total in the area sizes that are used in this investigation. Therefore it is chosen to use the same distances between the patches in flow direction ($L_{fbetween}$) as the transverse free spaces. Although total adaptation does not happen in these situations, different portions of the total adaptation length will be taken into account. In this way the influence of the adaptation length, although a part of it, on the aggregate roughness can be investigated. Table 4 gives the dimensions of the free spaces between the patches for the different pattern types and the pattern codes that are used.

Number of patches	Pattern code	$W_{fbetween}$ [m]	$L_{fbetween}$ [m]
2	21	-	60
	22	-	120
	23	60	-
	24	120	-
4	41	60	60
	42	120	60
	43	60	120
	44	120	120
9	91	60	60
	92	120	60
	93	60	120
	94	120	120

Table 4: Dimensions in meters of the smooth space between rough patches.

To be able to understand what the influence of a total adaptation of the flow is on the aggregate roughness, a couple of situations are used with a longer area: 1000 by 6000 m. The influence of one adaptation length will be investigated and therefore two patches of rough vegetation are placed behind each other in flow direction. Multiple runs will be made, with different $L_{fbetween}$. Each time the patches are placed closer to each other in order to investigate the influence of one adaptation length, because it gets less and less space to evolve until eventually there is only one elongated patch left. Figure 19 gives the layout of these pattern changes.

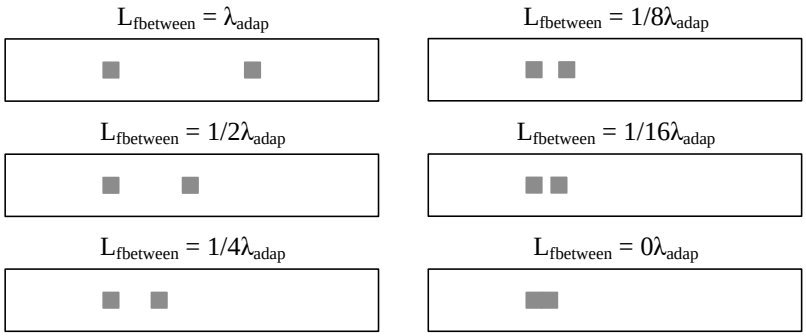

Figure 19: Examples of the pattern layouts where the $L_{fbetween}$ is varied per situation based on the λ_{adap}.

SERIAL ORIENTED

A total different pattern type is the serial pattern with a strip of rough vegetation placed transverse in flow direction. In this way there is no possibility for the flow to redirect and thus the total area is influenced by the pattern. Because it is not known for certain whether including more serial stripes will have a different effect than including one stripe, it is shortly investigated what is the case. After implementing three different patterns, one stripe, two stripes and three stripes, it can be concluded that implementing more stripes gives the same results as implementing one stripe. It will thus be enough to restrict the serial pattern to one stripe with rough vegetation.

COVERING

Other than the layout of the vegetation pattern which is discussed until now, also the covering of bushes on the area is a parameter that is taken into account. The covering of bushes can range from zero to hundred percent. In Appendix III the theoretical parallel and serial lines and the weighted method lines are plotted. The WAQUA results fall within the theoretical parallel and serial lines and the range is thus higher for lower coverings and smaller for higher coverings. Therefore more patterns with a lower covering will be used than with a high covering. Fifty, sixty, eighty and ninety percent will not be included because it is expected that that these will not give extra information than will be obtained using seventy percent together with ten till forty percent.

In table 5 the dimensions of the rough areas in the patterns are given. The W_p is given, but for the patterns with patches this is also L_p because the patches are squared. When more than one dimension is given this means that different dimensions are used in one pattern type. This is because it is tried to comply with the covering, and sometimes this means that the patches have to be of a different size. For example with a pattern with nine patches and a covering of 10 percent there are 7 patches with a W_p and L_p of 100 m and 2 patches with a W_p and L_p of 120 m.

Pattern type	W_p with 10% covering [m]	W_p with 20% covering [m]	W_p with 30% covering [m]	W_p with 40% covering [m]	W_p with 70% covering [m]
Parallel 1 strip	100	200	300	400	700
Parallel 2 strips	40 - 60	100 - 100	140 - 160	200 - 200	340 - 360
Parallel 3 strips	20 - 40 - 40	60 - 60 - 80	100 - 100 - 100	120 - 140 - 140	220 - 240 - 240
Patch 21 - 24	2x220	2x320	380 + 400	*	*
Patch 41 - 44	4x160	3x220 + 240	3x280 + 260	300 + 3x320	4x420
Patch 91 - 94	7x100 + 2x120	6x140 + 3x160	8x180 + 200	5x220 + 4x200	*

Table 5: Dimensions in meters of the rough vegetation areas per pattern type.

Also for the extra model calculations with a longer area where the total adaptation length can evolve four different coverings are used to be able to investigate whether the covering has an influence on the possible relation. But these do not comply with the coverings given in table 5 because the flow adaptation processes must be captured in total in the area of investigation. Therefore it is chosen to take four different patch sizes: 100x100 m, 200x200 m, 300x300 m and 400x400 m which is a covering of respectively: 0.0033, 0.013, 0.03 and 0.053 percent.

4.3 RESULTS OVERALL HYDRAULIC ROUGHNESS

In this paragraph the Chézy values obtained from the WAQUA calculation results are presented. These results will help in defining relationships between parameters and the aggregate Chézy value. The results are plotted together with the parallel and serial functions given in formula 1.4 and 1.5 respectively. In Appendix VI tables showing the discharge and aggregate Chézy roughness results are included. In the following, first the influence of the water depth on the aggregate roughness is investigated, followed by the grid size. After that the different patterns are handled which help to understand the influence of specific geometric characteristics of the vegetation pattern, for example the patch sizes. In paragraph 4.3.4 the influence of the general serial or parallel direction of the flow on the aggregate Chézy value is presented and at the end the prediction capability of the WA-method is investigated.

4.3.1 WATER DEPTH

As was already discussed in paragraph 4.2.2 three different water depths are used in the calculations in order to understand the impact of the water depth on the aggregate roughness value. In table 6 the Chézy values belonging to the vegetation is given per water depth. These are calculated using formula 4.1 given in paragraph 4.2.1.

	Water depth = 3 m	Water depth = 5 m	Water depth = 7 m
Grass	38.9 $m^{1/2}/s$	42.8 $m^{1/2}/s$	45.7 $m^{1/2}/s$
Bushes	0.7 $m^{1/2}/s$	4.7 $m^{1/2}/s$	7.3 $m^{1/2}/s$

Table 6: Chézy values for grass and bushes for different water depths.

The Chézy values thus increase when the water depth increases, which means that the vegetation is less rough. In figure 20 three figures are included with the aggregate Chézy values plotted against the covering of bushes on the area. The left figure shows the results for 3 m water depth, the middle figure for 5 m and the right figure for 7 m water depth. All the patterns types are included in these figures.

It is apparent that the aggregate Chézy values increase when the water depth increases and thus show the same distribution as in table 6. Most of the results show the same dependence of the results to the covering. The only exceptions are the results with the lowest Chézy values. After a closer look at the results it turns out that these results belong to the complete serial patterns. When the water depth increases the dependence of the aggregate Chézy value of the serial patterns changes, the aggregate Chézy values increase compared to the aggregate Chézy values of the other patterns.

It can be concluded that the water depth does have an influence on the aggregate roughness of the area; an increasing water depth leads to larger aggregate Chézy values.

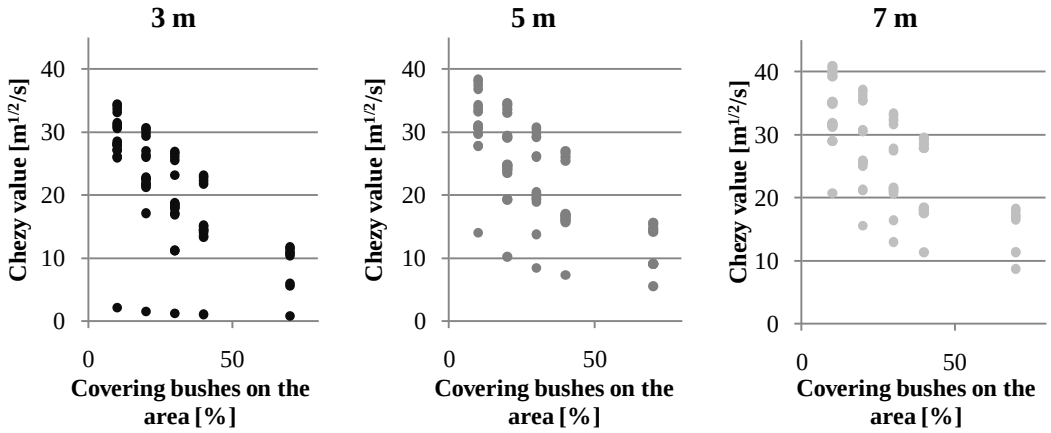

Figure 20: The aggregate Chézy values of all the pattern types plotted per water depth. From left to right: 3 m, 5 m and 7 m.

4.3.2 GRID SIZE

In the calculations also a distinction is made between grid cell sizes in order to investigate whether this will influence the flow properties and thus the aggregate roughness of the area. In figure 21 the chart containing the results of using a 10 m grid cell size (black points) and 20 m grid cell size (grey points) is included. It is obvious that the results are almost similar and using one grid size or another will not considerable alter the results. Using a smaller grid size does negatively influence the calculation time and the size of the output files and is thus not desirable to use. This conclusion also justifies the use of 20 m grid cells in the remaining model runs.

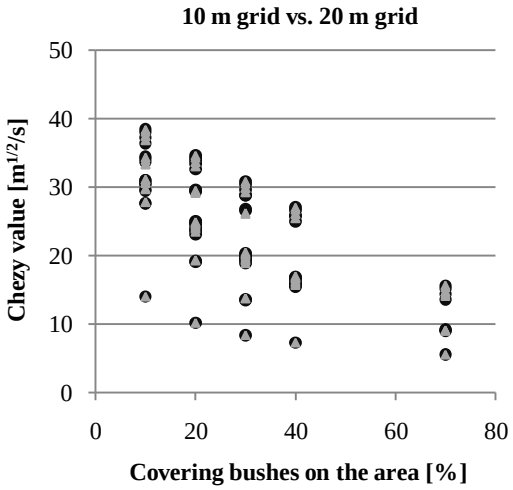

Figure 21: Comparison between the results using 10 m grid and 20 m grid size

4.3.3 PATTERNS AND COVERAGE

In this sub paragraph the influence of the geometrical dimensions of the vegetation patterns on the aggregate Chézy roughness is tried to be determined. First the parallel patterns are discussed followed by the patterns that contain squared patches. By doubling the space between the patches of bushes the influence of this geometrical parameter can be determined. The focus will lie on the model runs with a water depth of 5 m, because in paragraph 4.3.1 it was concluded that the water depth does not much influences the relative differences between the results.

4.3.3.1 PARALLEL PATTERNS

In figure 22 the aggregate Chézy values of the parallel patterns are plotted. All the coverings show the same distribution between the different parallel patterns; with one stripe on the side of the area (Par4) gives the highest Chézy value followed by the situation in where there is one stripe in the middle of the area (Par1). Including more and more stripes, and thus making the pattern division more spread, makes the aggregate Chézy value lower, and thus an averagely rougher situation.

The parallel patterns Par2-2 and Par3-2 are not included because the aggregate roughness was almost equal to the patterns Par2 and Par3. This indicates that when not the whole mixing layer can develop this does not influence the aggregate roughness much.

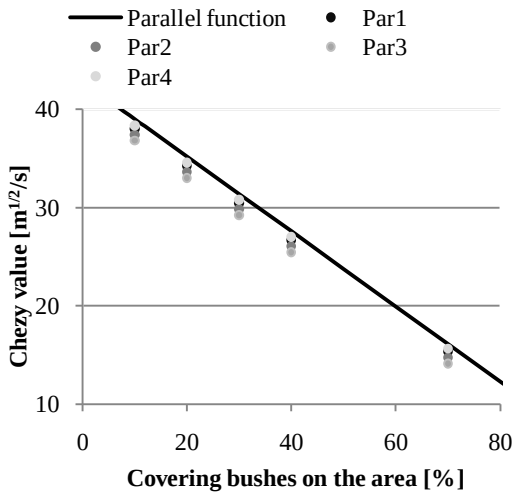

Figure 22: The aggregate Chézy values on an area with a parallel pattern plotted against the covering of bushes. The pattern belonging to Par1, Par2 etc can be found in Appendix V.

The total width of the rough vegetation and the total width of the smooth vegetation are more split up when the amount of stripes increases but the dimensions remain equal. Therefore the actual difference between the patterns is the amount of transitions from smooth to rough perpendicular to the flow direction. In chapter 3 it is explained that there is a mixing layer above such a transition and thus an increasing number of mixing layers means that a larger area is influenced by mixing widths.

In figure 22 it is not that clear to see the differences between parallel pattern types, therefore figure 23 is included. This figure shows the aggregate Chézy values plotted against the amount of mixing layers that are present (N_δ). The more mixing layers there are the lower the Chézy values get. The results that lay exactly above each other represent equal patterns but different coverings of bushes, the lower the aggregate Chézy value the higher the covering. It can thus be concluded that there is a consistent reduction in aggregate Chézy value when the number of smooth-rough transitions increases and that the covering does not influence this reduction.

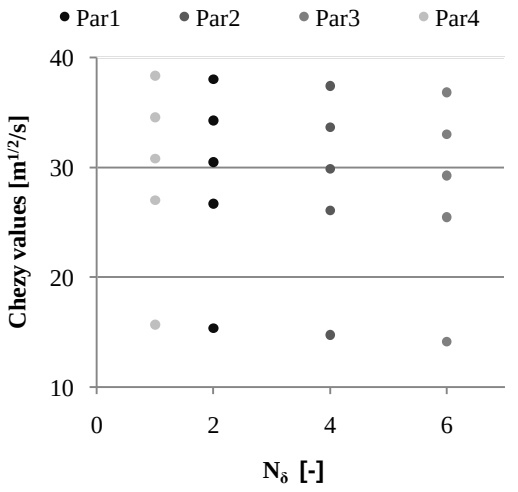

Figure 23: The aggregate Chézy values plotted against the number of mixing layers (N_δ).

4.3.3.2 PATCHES

The aggregate Chézy values on an area that has a vegetation pattern with different square patches are plotted in figure 24 together with the parallel and serial functions. The results lay between the parallel and serial function, the parallel function overestimates the Chézy values and the serial function underestimates the results. The aggregate Chézy values of an area with 2 patches show large differences, some lay closer to the parallel function and some are situated closer to the serial function. A closer look at the results reveals that the high values belong to the patterns that are parallel oriented to the flow direction and the low values to the serial oriented pattern. The aggregate Chézy values of the patterns with 4 and 9 patches show not much difference. These patterns are not particular serial or parallel oriented. This might indicate that the position in flow direction, serial or parallel, plays a large role in the aggregate roughness compared to the spreading of the patches because 4 or 9 patches do not give large differences in aggregate roughness values.

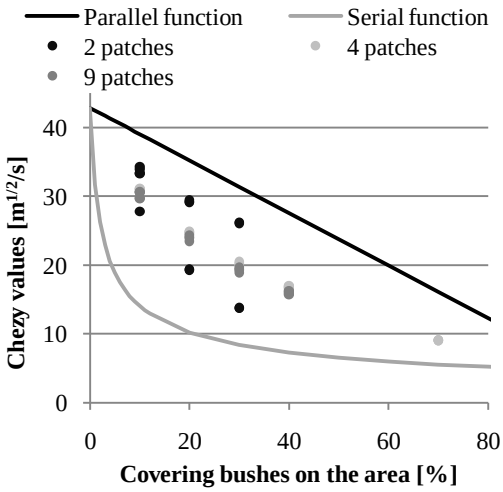

Figure 24: Aggregate Chézy values of patterns with patches plotted with the parallel and serial function.

The free space between the patches was also varied. This is done to investigate whether the amount of developed mixing layer and adaptation length will influence the aggregate Chézy value. By changing the free space a smaller or larger part of the mixing layer and adaptation length will be present. It turns out that these differences are minor. This indicates that not the exact dimensions of the pattern plays a role (which were thus varied between the patterns) but that the average dimensions (this includes also the covering, because the dimensions of the patches depend on this) and the parallel and serial direction of the pattern in the flow.

These two influences, the covering and direction in the flow, are clear in figure 24. The higher the covering the lower the aggregate Chézy values and the serial, parallel and square average patterns show large differences in aggregate Chézy values.

Both the mixing layer and the adaptation of the flow behind the patches play a role in these pattern types and induce an additional roughness. The influence of the mixing layer is already proven to exist in the former paragraph but the influence of the adaptation of the flow is not yet very clear using the results of the patches patterns. In Appendix VI-A the results for the model calculations with a water depth of 5 m and a grid size of 20 m are given. These results show minor differences between the different patterns, but these are not very clear probably because the amount of adaptation that can evolve is small compared to the total adaptation length.

The patterns with two patches have two complete different situations, as already discussed above. The serial oriented one has two large areas in where the adaptation of the flow takes place. These patterns give a much rougher area and this might indicate that the influence of the adaptation of the flow behind a patch has a larger influence than the mixing layer. Because only small parts of the adaptation behind the patch can evolve in the situations used a couple more simulations with a larger total area in order to let the adaptation length to be developed fully. Figure 25 shows the results of these model runs, in where the aggregate Chézy value is plotted against the ratio $L_{fbetween}/\lambda_{adap}$. $L_{fbetween}$ is the length of the free space between the patches. When this ratio is zero there is no space between the patches left; only one elongated patch and when this ratio is one, the adaptation of the flow can evolve completely before the flow reaches the following patch.

In figure 25 it can be seen that when the patch sizes increase, and thus the covering increases, the aggregate Chézy values decrease. But the situations where the patches stay of equal size the aggregate Chézy values also decreases when the ratio $L_{fbetween}/\lambda_{adap}$ increases. This indicates that there is a consistent influence of the ratio $L_{fbetween}/\lambda_{adap}$ on the aggregate roughness. This effect is also present at small ratios, as is used in all the situations in this study, but not as pronounced as seen in figure 25. These results thus help in understanding what the influence of the adaptation length is.

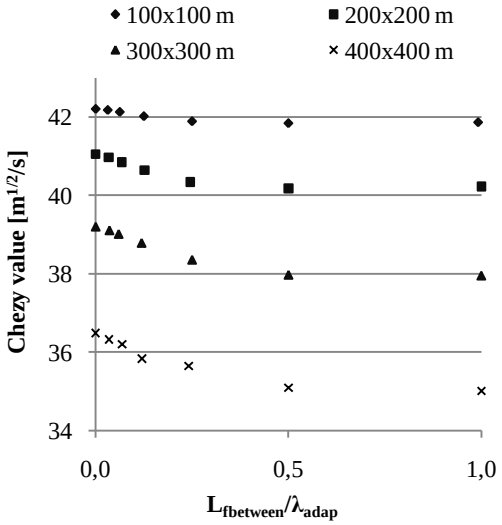

Figure 25: The aggregate Chézy values obtained using a large modeling area plotted against the ratio $L_{fbetween}/\lambda_{adap}$. Different patch sizes are used.

It can be concluded that also here the adaptation length and the mixing layer have an influence on the aggregate Chézy value next to the covering of the rough vegetation. This influence is dependent on the layout of the vegetation pattern.

4.3.3.3 SERIAL

The results of the aggregate Chézy values for the complete serial patterns are shown in figure 26 together with the serial function. The results lay exactly on the serial function and it is thus already possible to predict the aggregate Chézy values for a serial pattern.

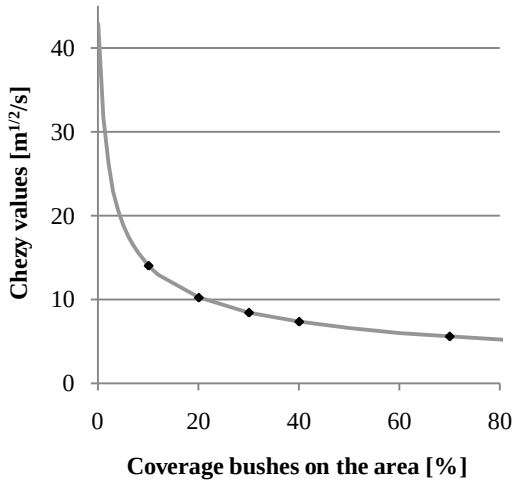

Figure 26: Aggregate Chézy values of serial patterns plotted together with the serial function

4.3.4 LAY OUT DIRECTION

In the last three paragraphs the aggregate roughness of the different types of patterns were discussed in which it was mentioned that the overall direction in the flow has a large influence on the aggregate roughness. This overall direction, parallel or serial, can be expressed as a ratio between the total length in flow direction of the rough vegetation ($\sum L_p$) and the total width of the rough vegetation ($\sum W_p$). $\sum L_p / \sum W_p$ can be seen as an expression for the amount of streamlining of the vegetation pattern.

In figure 27 the aggregate Chézy values of all the patterns discussed above are plotted against the ratio of $\sum L_p / \sum W_p$. If $\sum L_p$ is larger than $\sum W_p$ the direction is more parallel than serial and will thus give a higher aggregate roughness and if it is the other way round the direction is more serial and the aggregate roughness will be smaller. In figure 27 this trend is very clear.

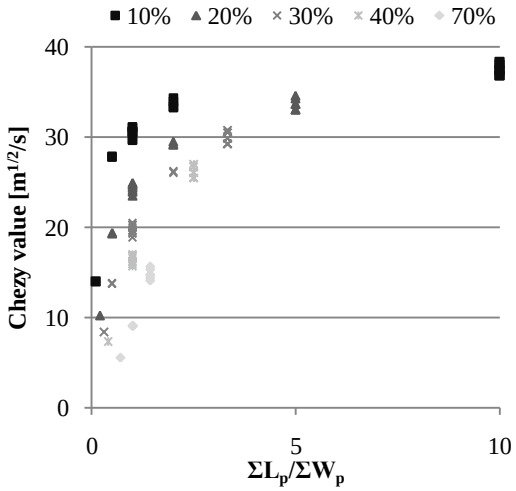

Figure 27: Aggregate Chézy values of all the patterns discussed in this paragraph plotted against the ratio $\sum L_p / \sum W_p$ which is the degree of streamlining of patterns.

When the covering of rough vegetation increases, the aggregate Chézy values decrease. But also the streamlining ratio decreases, this is for example in case of a parallel pattern because the total width

increases but the length of the patch stays equal for all the coverings (total length of the area, L_t). Therefore the effect of streamlining decreases with increasing covering due to the increasing width, but equal length for the parallel pattern. Figure 28 clarifies this effect.

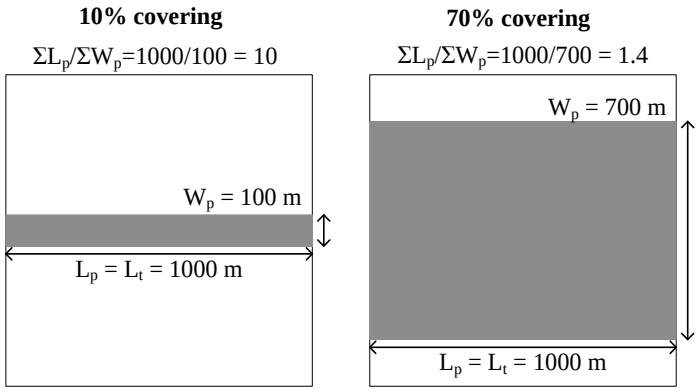

Figure 28: Parallel pattern with dimensions for 10 and 70 percent covering of rough vegetation.

This trend also indicates that the influence of the mixing layer is smaller than of the adaptation length on the aggregate roughness. Because when a pattern is averagely more serial oriented the adaptation length has a larger area available than when the average pattern is parallel oriented, this is especially clear with the pattern type that contains 2 patches.

4.4 COMPARISON WITH WA-METHOD

When the patterns that are used in this study are present in one grid cell in WAQUA than the WA-method will give a weighted Chézy value, the only exception is the serial pattern, which is predicted by the serial function. The results will thus be compared with the predicted values of the WA-method in order to investigate the accuracy of the method.

In figure 29 the Chézy values calculated with the WA-method are plotted against the Chézy values measured with WAQUA per water depth. The solid line indicates perfect agreement. Almost all the aggregate Chézy values are underestimated by the WA-method. With increasing water depth the predictions are getting a bit better. Especially the parallel pattern types are underestimated, followed by the pattern with two patches parallel oriented.

These figures show that the WA-method does not give very accurate predictions for the roughness of the vegetation patterns. In the next chapter it is tried to develop a new method which will be able to give more accurate predictions of the aggregate Chézy values.

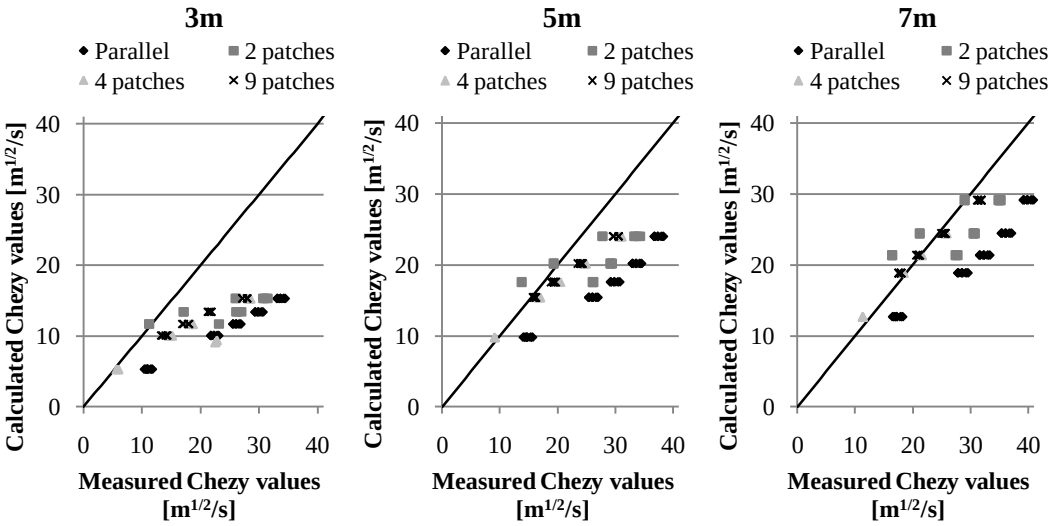

Figure 29: With the WA-method calculated Chézy values plotted against with WAQUA measured Chézy values. The solid line indicates perfect agreement.

5 A NEW PREDICTION METHOD

In the previous chapter it became clear that the flow characteristics mixing layer and flow adaptation length can help in describing the aggregate roughness on an area with different vegetation types. In this chapter a new method will be set up that predicts the aggregate Chézy values of a vegetation pattern. First the manner in which the new method is developed and the steps that have been followed will be explained. After this the new model will be compared with the now in use WA-method in order to investigate whether the use of the new method will give an improvement in accuracy. Then the behaviour of the new method is investigated and at the end of this chapter the new method is validated on a broader set of situations where the eddy viscosity coefficient, ratio of roughness and different vegetation patterns are changed compared to the situations on which the model is based.

5.1 DERIVATION

To be able to make a start with building up a method that will be able to predict the aggregate roughness based on the outline of the vegetation pattern a plot is used where all the results are shown with the serial and parallel functions, see figure 30. In this plot it can be seen that the parallel line overestimates all the aggregate Chézy values measured with WAQUA and that the serial line underestimates almost all, except the serial patterns, Chézy values. Furthermore the results show a more linear pattern than a curved one, and therefore it is chosen to start with the parallel line as starting point of the derivation.

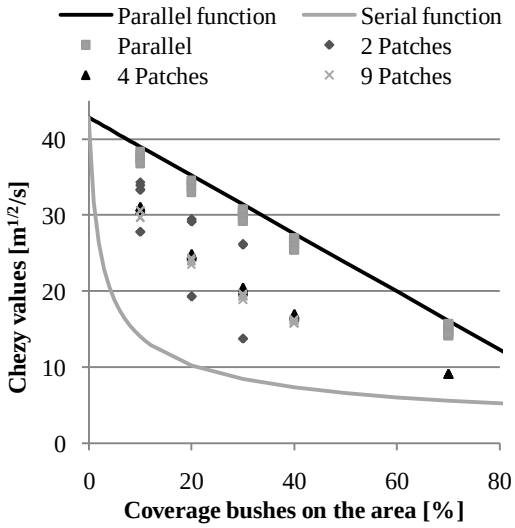

Figure 30: Plot with the aggregate roughness values obtained with WAQUA with the serial and parallel functions.

Because the parallel function overestimates all the aggregate Chézy values the following function can be made as base function:

$$C_a = C_p - C^* \qquad [5.1]$$

In where C_a is the aggregate Chézy value of the area, C_p is the parallel function and C* represents the additional roughness that is induced by the vegetation pattern that is not taken into account with only the parallel part of the function. Written out this function can also be expressed as:

$$C_a = x_r C_r + (1 - x_r) C_s - C^* \quad [5.2]$$

With:

C_r	= Chézy value belonging to rough vegetation	[$m^{1/2}/s$]
C_s	= Chézy value belonging to smooth vegetation	[$m^{1/2}/s$]
C*	= Additional roughness	[$m^{1/2}/s$]
x_r	= Area fraction rough vegetation	[-]

The area fraction can be expressed as a function dependent on the dimensions of the vegetation pattern. When is assumed that the different square rough patches are of equal size on the area the fraction can be expressed as follows:

$$x_r = \frac{N_p \cdot L_p \cdot W_p}{W_t \cdot L_t} \quad [5.3]$$

With:

N_p	= Number of rough patches	[-]
L_p	= Length of rough patches	[m]
W_p	= Width of rough patches	[m]
W_t	= Width of total area	[m]
L_t	= Length of total area	[m]

In order to deduce C* different steps are taken. First, in the next sub paragraph, the parallel patterns are used in order to deduce the first part for C*. Here only the mixing width is responsible for the additional roughness. After that influence on the additional roughness of the adaptation of the flow behind the patches is used in order to deduce the second part of C*.

5.1.1 ADDITIONAL ROUGHNESS: MIXING LAYER WIDTH

To make a start in defining the parameters that should be used to define C* an easy pattern lay out is used as a first start, namely the parallel pattern in the situation with 5 m water depth. This pattern consists of lanes with different Chézy values that extent over the entire length of the area. A mixing layer is present above the smooth-rough transitions. This mixing layer is the only process happening with this pattern type that influences the additional roughness, which is thus easy to grasp. In figure 30 the aggregate Chézy values of the parallel patterns are marked with square points. In figure 31 these three parts are shown.

The deviation between the parallel function and the different parallel patterns is caused by the number of mixing layers, and thus transitions from smooth to rough and vice versa perpendicular to the flow direction. The more transitions there are the more the aggregate Chézy value obtained with the model deviates from the parallel function. From this it can be deduced that the mixing width (δ) and the number of mixing widths (N_δ) are two of the parameters that needs to be included in the function.

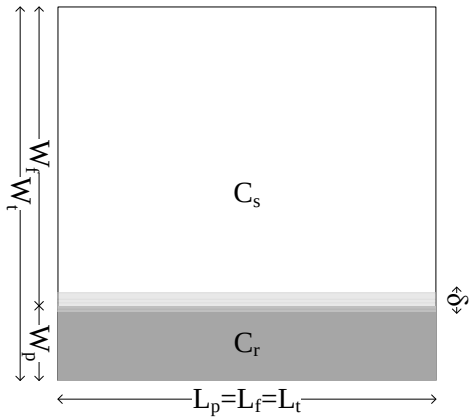

Figure 31: Parallel pattern showing the properties of the pattern.

The parallel function is based on the area division of C_s and C_r. The influence of the mixing layer can also be seen as an additional area division. It is named additional on purpose, because the areas for C_s and C_r will not get smaller when the area of the mixing width is included. It is an additional roughness that is included and thus the area should not be seen as a real area but as a roughness that is laid on the already existing area. The total area of the mixing width is the width multiplied with the length of the patch, in the case of the parallel pattern the total length of the area, when this area is divided by the total area the share of the mixing width is expressed in area division. This gives the L_p and the A_t (total area) as another two extra parameters.

At this point four parameters are deduced based on the layout of the parallel pattern and the influence that the pattern has on the flow (δ). But these parameters are all dimensional parameters and a Chézy value needs to be the outcome of the function. Therefore the assumption is made that the aggregate Chézy value of the mixing width is the average value of C_s and C_r.

Now that all the parameters are defined the function can be set up:

$$C_\delta^* = \alpha_1 f(\overline{C}, A_\delta, A_t) \quad [5.4]$$

With:

$$\overline{C} = (C_s + C_r)/2 \quad [5.5]$$

$$A_\delta = \delta \cdot L_p \cdot N_\delta \quad [5.6]$$

$$A_t = L_t \cdot W_t \quad [5.7]$$

The function needs to calculate the additional roughness that is induced by the mixing widths, and thus the dimension must be the same of the Chézy value, to comply with this the following function can be deduced:

$$C_\delta^* = \alpha_1 \overline{C} \cdot \frac{A_\delta}{A_t} = \alpha_1 \frac{C_s + C_r}{2} \cdot \frac{\delta \cdot L_p \cdot N_\delta}{L_t \cdot W_t} \quad [5.8]$$

Formula 5.8 can be rewritten using formula 5.3 in:

$$C_\delta^* = \alpha_1 \frac{C_s + C_r}{2} \cdot x_r \cdot \frac{\delta \cdot N_\delta}{W_p \cdot N_p} \quad [5.9]$$

This additional roughness is thus dependent on the ratio between the total width of the mixing layers ($\delta \cdot N_\delta$) and the total width of the rough vegetation ($W_p \cdot N_p$).

To determine the value of the constant α_1 the predicted aggregate Chézy values are compared with the measured values in WAQUA. First here the error sum of squares will be used for this. This quantity gives a measure of the deviations between the measured and calculated values. The formula to calculate the error sum of squares is (Davis, 2002):

$$SSe = \sum_i (y_i - f_i)^2 \quad [5.10]$$

With:

y_i = The measured Chézy values for pattern i [$m^{1/2}/s$]

f_i = Predicted Chézy value for pattern i [$m^{1/2}/s$]

In chapter 3 the influence of the water depth and eddy viscosity on the mixing layer width is discussed. The mixing layer widths for the different water depths (40 m for 3 and 5 m water depth and 60 m for 7 m water depth) are included. The average Chézy value is constant, because only two roughness types are used. The other parameters are different per vegetation pattern. It turns out that a value for α_1 of 0.38 gives the best results. In order to see this in figure 32 the measured Chézy values are plotted against the predicted Chézy values. It can be seen that the results lay almost perfectly on the black line, which indicates that the predicted values almost match the measured values. The total SSe for this value is 0.84.

At this moment the formula to predict the aggregate Chézy value for a parallel pattern is as follows:

$$C_a = x_r C_r + (1 - x_r) C_s - 0.38 \cdot \frac{C_s + C_r}{2} \cdot x_r \cdot \frac{\delta \cdot N_\delta}{W_p \cdot N_p} \quad [5.11]$$

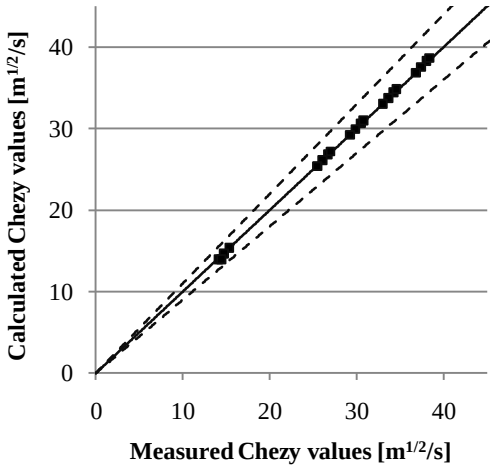

Figure 32: Calculated Chézy values plotted against the measured Chézy values of the parallel pattern with a water depth of 5m. The solid line indicates perfect agreement and the dotted lines the 10 percent range.

5.1.2 ADDITIONAL ROUGHNESS: FLOW ADAPTATION BEHIND ROUGH PATCH

Now that the aggregate Chézy roughness of a parallel pattern can be predicted this can be used to expand the prediction method to patterns were also the adaptation length plays a role. To make a first start again one pattern type is taken as first exploration (results with water depth of 5 m), the serial oriented pattern with two patches. It might seem more logical to take the complete serial pattern, but it is already possible with the serial function to predict the aggregate roughness of these patterns and therefore these types are not used in the derivation of the new prediction method. In figure 30 it can be seen that the other patterns have a lower Chézy value than the Chézy values belonging to a parallel pattern. Therefore the same steps will be taken as in the former paragraph but this time the adaptation length is the flow characteristic that induces the additional roughness (the influence of the mixing width is already described in the first part of the formula).

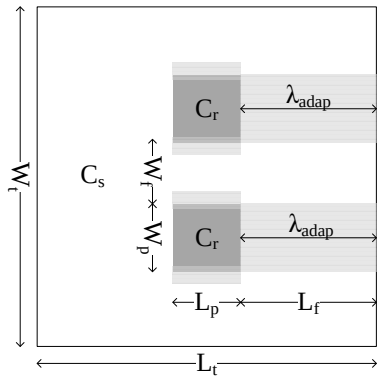

Figure 33: Pattern with two serial oriented patches. The properties of this pattern are shown.

In figure 33 the dimensions of the pattern are shown. Some assumptions have been made, first of all the adaptation length will be seen as a squared block instead of a sort of triangle where the width of the adaptation decreases. Secondly the mixing width is also seen as a squared block and thirdly only these

two flow characteristics are taken into account, the other, for example before the patch, are assumed not to have an influence on the aggregate Chézy value. Also the average Chézy value in the block of the adaptation length is the average of C_s and C_r.

Again it is assumed that the additional roughness induced by the adaptation length can be seen as an extra area laid on the existing area with a width the same as the width of the patch. The adaptation length however cannot be assumed to be constant because it varies with patch width. Therefore the average free length behind the patch should also be taken as a parameter (because also the length behind the pattern plays a role). The proportion $\overline{L_f}\backslash\lambda_{adap}$ has to be used in order to define the length of the adaptation area. However if this proportion is larger than 1, this means that the total adaptation length can evolve, but this does not mean that more than one adaptation length is present and therefore a minimum function is needed to make sure that the proportion never exceeds the value of one. The formula to calculate the adaptation length is deduced in chapter 3.

Taking the proportion L_f/λ_{adap} is also needed in order to let this additional roughness be zero in case of a parallel pattern, the parallel pattern can already be predicted with the first part of the additional roughness (induced by δ) and therefore the second part should be zero. But because there is no L_f in case of a parallel pattern, this second part will be zero in total and thus rules out in case of a parallel pattern.

Because in this situation L_p is not equal to L_t, one extra assumption has to be made; namely that the C^*_δ is also applicable when $L_p < L_t$. In this situation also more patches can be present on an area. The situations used in this study all have squared patches with almost all the same sizes (some exceptions were made in order to comply with the covering) therefore the dimensions for patches and free spaces will be average dimensions.

Taking the above together the following can be said:

$$C_a = \sum_i x_i C_i - 0.38 \cdot \frac{C_s + C_r}{2} \cdot x_r \cdot \frac{\delta \cdot N_\delta}{\overline{W_p} \cdot N_p} - C_\lambda^* \qquad [5.12]$$

With:

$$C_\lambda^* = \alpha_2 \cdot f\left(\overline{C}, A_\lambda, A_t\right) \qquad [5.13]$$

With:

$$\overline{C} = (C_s + C_r)/2 \qquad [5.14]$$

$$A_\lambda = \lambda_{adap} \cdot \overline{W_p} \cdot N_p \cdot min\left(1, \frac{\overline{L_f}}{\lambda_{adap}}\right) \qquad [5.15]$$

$$A_t = L_t \cdot W_t \qquad [5.16]$$

The same sort of function as is deduced in the former paragraph can be deduced with the use of the above properties, namely:

$$C_\lambda^* = \alpha_2 \overline{C} \frac{A_\lambda}{A_t} = \alpha_2 \frac{C_r + C_s}{2} \frac{\lambda_{adap} \cdot \overline{W_p} \cdot N_p \cdot min\left(1, \frac{\overline{L_f}}{\lambda_{adap}}\right)}{L_t \cdot W_t} \quad [5.17]$$

Formula 5.17 can be rewritten using formula 5.3 in:

$$C_\lambda^* = \alpha_2 \frac{C_s + C_r}{2} \cdot x_r \frac{\lambda_{adap} \cdot min\left(1, \frac{\overline{L_f}}{\lambda_{adap}}\right)}{L_p} \quad [5.18]$$

When the flow adaptation cannot evolve fully the additional roughness is dependent on the ratio L_f/L_p. When the flow adaptation is fully present in the area the additional roughness is dependent on the ratio L_{adap}/L_p

The parameter α_2 needs to be determined using the measured aggregate Chézy values with WAQUA of the patterns which contain two patches that are serial oriented. Again the SSe is used to determine the most optimal α_2. This parameter however needs to be refined later on when all the patterns are used, for this time it is only deduced in order to check whether the formula for $C_{extra,\lambda}$ is able to predict the additional roughness.

Using the calculations with 2 serial oriented patches a value of α_2 of 2.93 gives the minimal value for SSe, namely 2.80. In figure 34 the measured Chézy values are plotted against the predicted Chézy values. It can be seen in this figure that this function is able to predict the aggregate Chézy value pretty well when both the adaptation length and the mixing width induce an additional roughness.

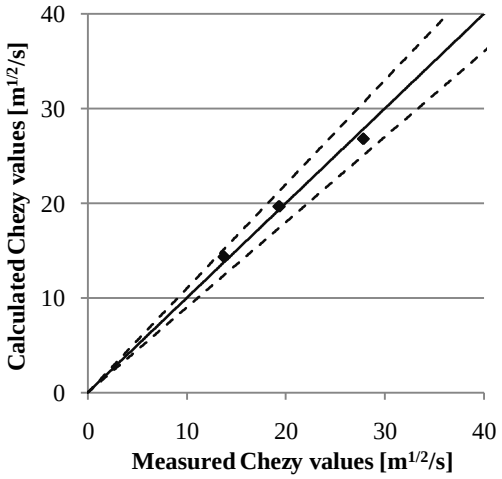

Figure 34: Calculated Chézy values plotted against the measured Chézy values of the serial oriented pattern. The solid line indicates perfect agreement and the dotted lines the 10 percent range.

5.1.3 INCLUDING ALL PATTERN TYPES

In the previous two paragraphs the prediction method is deduced based on a selection of vegetation patterns. In this paragraph all pattern types are included, except the complete serial pattern. The SSe will not be used anymore to see how accurate the method works. Instead the percentage of the predicted Chézy values that fall within the 10 percent deviation range is used. This is done because it is

assumed to be of more importance that most predictions fall within this range than an averagely better prediction with some large deviations.

With the value of 2.93 for α_2 87.2 percent of the results of the 5 m water depth runs fall within the 10 percent deviation range. After changing this factor to 2.62 more values fall within the range; 97.7 percent. The value of α_2 will thus be adapted to 2.62. Formula 5.13 gives the end result.

$$C_a = x_r C_r + (1 - x_r) C_s - \frac{C_r + C_s}{2} \cdot \left[0.38 x_r \cdot \frac{\delta \cdot N_\delta}{\overline{W_p} \cdot N_p} + 2.62 x_r \cdot \frac{\lambda_{adap} \cdot min\left(1, \frac{\overline{L_f}}{\lambda_{adap}}\right)}{L_p} \right] \qquad [5.19]$$

Rewriting formula 5.19 in a different way gives:

$$C_a = C_s - x_r C_s [1 + \gamma] + x_r C_r [1 - \gamma] \qquad [5.20]$$

With:

$$\gamma = 0.19 \frac{\delta \cdot N_\delta}{\overline{W_p} \cdot N_p} + 1.31 \frac{\lambda_{adap} \cdot min\left(1, \frac{\overline{L_f}}{\lambda_{adap}}\right)}{L_p} \qquad [5.21]$$

Mind in formula 5.21 the values that were obtained using the results of the WAQUA computations are divided by two, resulting from $(C_r+C_s)/2$.

In figure 35 the measured Chézy values are plotted against the predicted Chézy values. The prediction is very accurate, and almost all patterns fall within the 10 percent confidence line. The crosses fall outside the ten percent line, which represents the results of the pattern with 2 patches. For these patterns a larger Chézy value is predicted than was measured. After taking a closer look at the patterns it turns out that these particular ones represent the 2 patches that are serial oriented. This pattern type is the only very distinct serial oriented pattern, because the complete serial patterns are not predicted with this new model. This may indicate that a serial pattern induces more disturbances around the roughness transitions than the other, on average more square, patterns do. The parallel patterns however, and thus the influence of the mixing width, can very well be described by the new model, which gives the impression that the deviation of the serial oriented pattern is induced by the adaptation of the flow behind the patches.

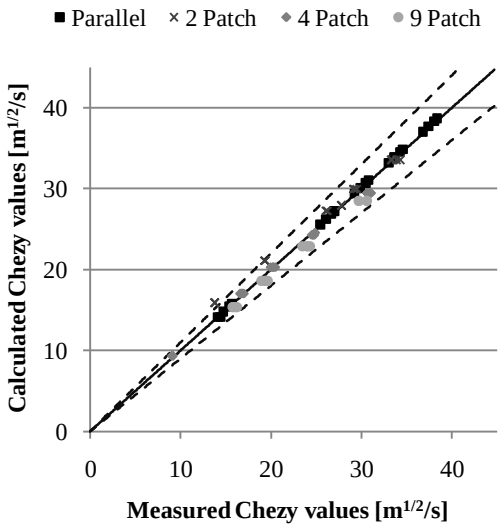

Figure 35: Calculated Chézy values plotted against the measured Chézy values of all the patterns with a water depth of 5m. The solid line indicates perfect agreement and the dotted lines the 10 percent range.

In Appendix VII the same plots are given for the other water depths. From this it can be concluded that the method is also applicable for different water depths. In table 7 the percentage of the results that falls within the 10 and 5 percent range of the measured results are shown. Almost all the results fall within the 10 percent deviation range and more than 75 percent within the 5 percent range; a very good result.

Water depth [m]	10% range	5% range
3	94,2%	82,6%
5	97,7%	88,4%
7	97.7%	75.6%

Table 7: The amount of predicted Chézy values that fall within the 10 and 5 percent deviation range.

As already stated above the serial patterns are predicted here with the serial formula:

$$C_s = \frac{1}{\sqrt{\sum_i \frac{x_i}{C_{ri}^2}}} \qquad [5.22]$$

The use of this formula gives a better representation of the measured Chézy values than the use of the new model. The new model can be used to predict the aggregate roughness but is less accurate. In figure 36 this can be seen. The grey points are the Chézy values predicted by the serial formula given in formula 5.22 and all fall within the ten percent confidence line and they all seem to lay almost perfect on the optimal line. The black points are the Chézy values predicted by the new method and are not that accurate; almost none of the values falls within the ten percent confidence line which means that the values are not very accurate predicted. That is why it is chosen to predict the aggregate roughness of a serial pattern with the serial formula instead of the new method.

When to make use of the new prediction model or the serial function depends on whether the pattern is completely serial. A pattern is completely serial when W_p/W_t is 1. Thus when this ratio is smaller than 1 the new prediction model has to be applied.

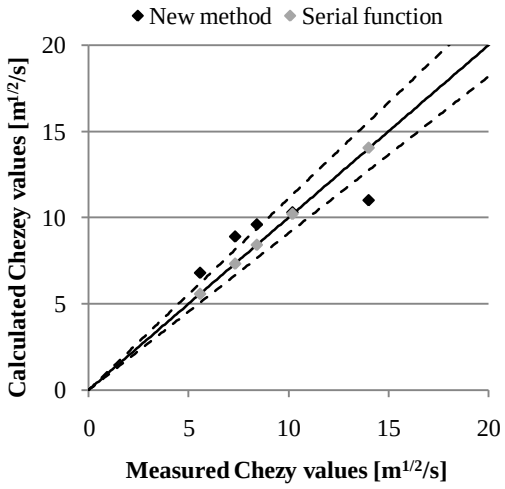

Figure 36: Comparison of the results of the serial pattern predicted by the new model (black points) and by the already existing serial formula (grey points). The solid line indicates perfect agreement and the dotted lines the 10 percent range.

5.2 COMPARISON WITH WA-METHOD

The prediction method that is used at this moment in WAQUA is the WA-method (see chapter 1). In this paragraph the prediction capability of this WA-method is compared with the prediction capability of the new prediction model.

In figure 37 the results can be found for the runs with a water depth of 5 m. The black dots represent the results of the new model and the grey dots the results of the WA-method. It can be seen that the WA-method under predicts almost all Chézy values, which means that the aggregate roughness is predicted too rough. In this figure it is clear that for one covering only one Chézy value is predicted because the grey dots make horizontal lines in the figure. The new model however takes more distinct parameters of the pattern in account, which means that different patterns with an equal covering of rough vegetation will get different aggregate Chézy values. Against 97.7% of the results of the new model that falls within the 10% range only 25.6% of the WA-method falls within this range. It is thus clear that the new prediction method based on characteristics of the vegetation pattern is better capable in predicting the aggregate roughness of a vegetation pattern.

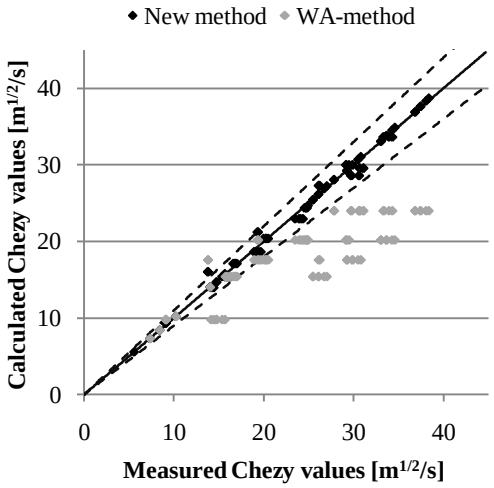

Figure 37: Comparison of the new prediction model (black points) and the now in use WA-method (grey points). The solid line indicates perfect agreement and the dotted lines the 10 percent range.

5.3 BEHAVIOUR OF THE MODEL

In this paragraph the behaviour of the new prediction method is investigated. This is done by taking one situation as basic assumption and then one parameter is varied in order to investigate how the model handles with this variation.

First a parallel pattern is taken in which there is one rough vegetation strip in the middle (par1), meaning two mixing layers. The basic situation has a water depth of 5 m, eddy viscosity of 0.5 m^2/s and bushes and grass as vegetation types, which are the black dots in figure 38.

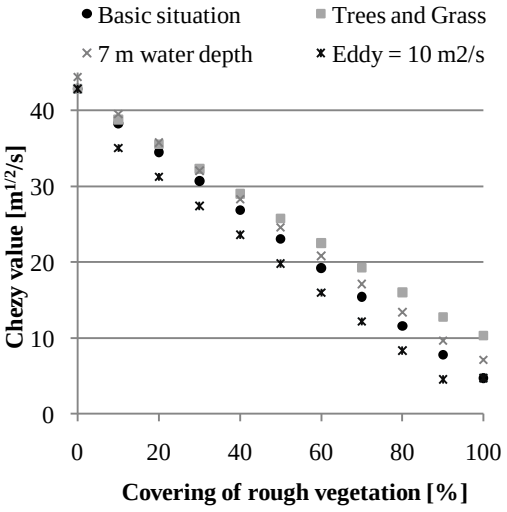

Figure 38: Chézy values belonging to a parallel pattern plotted against the covering of rough vegetation. The water depth, roughness ratio and eddy viscosity value is varied to investigate the behaviour of the method.

The method shows normal behaviour in almost all cases, the Chézy values are larger with a larger water depth, but also with a smaller roughness ratio, which is in this case grass with trees (C = 10.33

$m^{1/2}/s$). There is one abnormal point at the 90 percent covering. The predicted value with an eddy viscosity coefficient of 10 m^2/s is lower than the Chézy value of only bushes, which is not possible. This is because with increasing covering the width of the parallel rough vegetation stripe gets larger, in the case of 90 percent 900 m. The total width of the area is 1000 m en thus on both sides there is smooth vegetation with a width of 50 m left. With an eddy viscosity value of 10 m^2/s the mixing layer width is 220 m (see figure 9). This does not fit in the free width of grass, but this total width is taken fully in the method which leads to an over prediction of the additional roughness induced by the mixing layer.

The same sort of analysis is carried out with a pattern including four rough patches where both the mixing layer and the flow adaptation behind the patches induce an additional roughness. In figure 39 the predicted Chézy values are given. In this case, were also the flow adaptation at the lee side of a patch induces an additional roughness, the dependence with the covering is not linear but the gradient is strong at low coverings and reduces at higher coverings. This is because already with a small patch of rougher vegetation the flow adjustment processes are large. The model is thus capable of showing this relation.

Furthermore the situations where the water depth is larger and the roughness ratio is smaller the aggregate Chézy values are larger predicted compared to the basic situation. However when the eddy viscosity coefficient is increased towards 10 m^2/s, which gives a mixing layer of 220 m instead of 40 m the Chézy values are predicted too low for the high covering situations, even below zero which is not possible. This has already been observed at the parallel pattern results but in this situation it is more pronounced. The cause however is the same, but in this situation there are eight mixing layers implemented, of which the additional roughness are all over predicted because the mixing layers do not fit in the area.

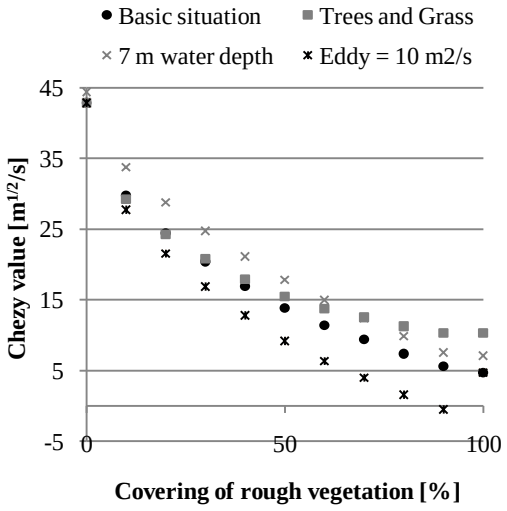

Figure 39: Chézy values belonging to a pattern with four square patches plotted against the covering of rough vegetation. The water depth, roughness ratio and eddy viscosity value is varied to investigate the behaviour of the model.

From this model behaviour it can thus be concluded that with a high covering, higher than 70 percent, and a high eddy viscosity coefficient the effect of the mixing width induces a too large additional roughness. In these extreme situations the model cannot be used in this form. This problem can be solved by also introducing a minimum function just like is implemented for the flow adaptation. If the ratio $\overline{W_f}/\delta$ (with $\overline{W_f}$ is the average smooth width) is smaller than one not the whole width of the mixing

layer can evolve and can thus also not fully induce the additional roughness. But this needs further investigation.

5.4 BROADER APPLICATION

In this chapter a new prediction method has been deduced. However until this point it is only applicable in the situations on which the model has been based. In this paragraph the application will be tested on a broader scale, with different patterns as used with the deduction of the model, a different eddy viscosity and with a different ratio between the two roughness values. It will be shortly investigated whether the model is still applicable in the same form, or that the parameters α_1 and/or α_2 should be changed in order to increase the prediction capability.

5.4.1 DIFFERENT PATTERNS

In the report of Van Velzen & Klaassen (1999) six different vegetation patterns were made in order to, in that time, deduce the WKS-method (see chapter 1). Instead of patterns where the patches lay perfectly next and behind each other, as where used in this study, they made irregular patterns, four with square patches and two with elongated patches. The water depth was 5 m and also the area size and slope were equal, thus the only difference is the layout of patterns of vegetation. In Appendix II the patterns are included.

In figure 40 the results are shown. The black dots show the results calculated with the new model. They almost all lay within the 10 percent range which is a good result. The grey dots are the results obtained with the WA-method, which is based on these patterns (see chapter 1). These dots lay almost on a horizontal line, which indicates that the Chézy values for the different patterns are almost equal when predicted by the WA-method, while the measured values are different.

It can thus be concluded that also other patterns, with the same eddy viscosity coefficient and the same roughness ratio, can very well be predicted by the new model.

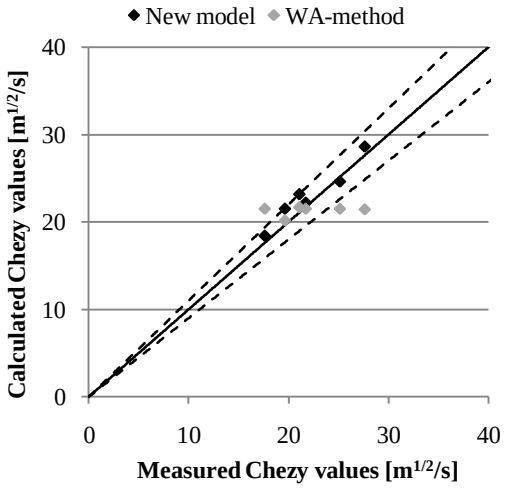

Figure 40: Comparison of the new prediction model (black points) and the now in use WA-method (grey points) for other patterns than are used during the derivation of the new prediction model. The solid line indicates perfect agreement and the dotted lines the 10 percent range.

5.4.2 EDDY VISCOSITY

Already in the beginning of this report the influence of the eddy viscosity has been discussed. The larger the eddy viscosity the wider the mixing layer will be. This means that the additional roughness that is induced by the mixing width will change when a different eddy viscosity will be used in the model. Therefore it is investigated whether the new prediction model can also be used with different eddy viscosity coefficients.

In chapter 3 the influence of the eddy viscosity coefficient is explained and it was concluded that with an increasing eddy viscosity value the mixing width increases, with a dependence $\delta \sim \sqrt{\varepsilon}$. Thus with a different eddy viscosity value in WAQUA the value of δ needs to be changed in order to comply with the wider or smaller mixing layer. Because in the handbook of WAQUA a default value of 10 m^2/s will be used as eddy viscosity coefficient when no value is given, it is tried to vary a parameter in the new model in order to comply with these types of situations. Because at the start of the process of making model runs with WAQUA an eddy viscosity coefficient of 10 m^2/s was used instead of 0.5 m^2/s a lot of results are present with this eddy coefficient. In order to predict the aggregate Chézy value of the area a value of 220 m should be taken for δ, see figure 9.

In figure 41 the results are plotted, but the overall accuracy is not as high as the results obtained in paragraph 6.2. The percentage that falls within the 10 percent range is 73 percent and 60 percent within the 5 percent range. This is higher than the accuracy of the WA-method (grey points) of which 32 percent falls within the 10 percent range and 16 percent within the 5 percent range.

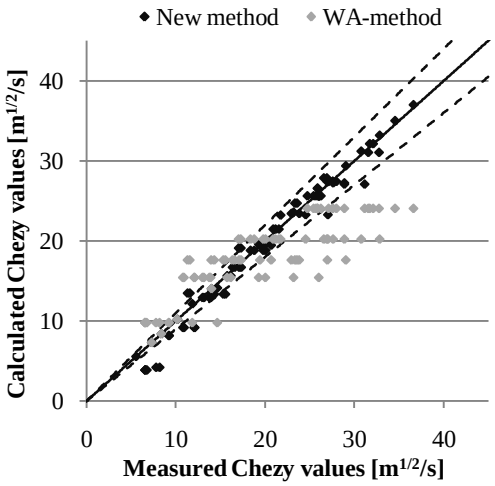

Figure 41: The calculated Chézy values are plotted against the measured Chézy values when the eddy viscosity coefficient is 10 m^2/s. The solid line indicates perfect agreement and the dotted lines the 10 percent range.

This change in eddy viscosity is also checked with the patterns that are made by Van Velzen & Klaassen (1999), see figure 42. The black points are the results obtained with the new model, and they all fall within the 10 percent range. The grey points are created with the WA-method and almost all fall outside the 10 percent lines. This indicates that the new method is also accurate in predicting the aggregate Chézy values when different patterns and a different eddy viscosity coefficient are used in the model WAQUA than the situations the new model is based on.

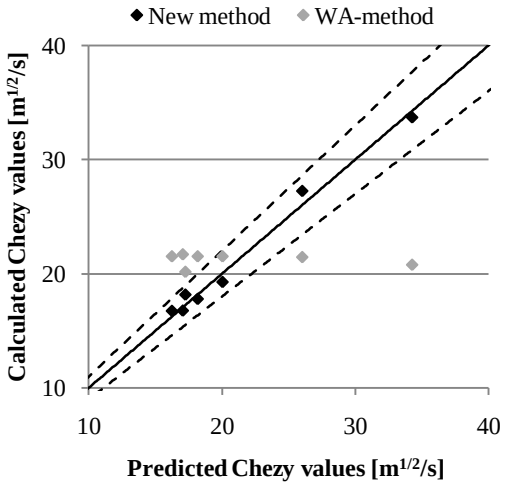

Figure 42: Comparison of the prediction capability of the new model (black dots) and the WA-method (grey dots) for irregular patterns created by Van Velzen & Klaassen (1999) and an eddy viscosity of 10 m^2/s. The solid line indicates perfect agreement and the dotted lines the 10 percent range.

5.4.3 ROUGHNESS RATIO

The measured aggregate Chézy values with WAQUA are all combinations of two types of vegetation roughness, grass and bushes. Because these two are very different; grass is very smooth and bushes are very rough, it is investigated whether the new method is also applicable when this ratio is not that large. Therefore the runs with 20 percent covering of bushes are repeated but instead of taking the roughness of bushes, the roughness of trees are used which has a Nikuradse roughness value of 16 m which is 10.33 $m^{1/2}/s$ Chézy roughness for a water depth of 5 m. The ratio between grass and trees is thus smaller and will result in larger aggregate Chézy values because averagely the area is smoother.

Due to this different ratio of roughness values the influence of the flow adaptation processes discussed in chapter 3 will be influenced. This is because the differences in flow velocities above the smooth and rough vegetation will decrease. Because of the already rather small mixing width of 40 m which means 2 grid cells when a grid size of 20 m is used, it is assumed that this width will not change. The change thus needs to be made in the part in where the adaptation length is handled. But when the free space between patches is smaller than the adaptation length, only this length is taken into account. Only when this free space is longer than the adaptation length, this length will be used in the formula. Therefore changing the formula for λ_{adap} will not give different solutions when the free space is shorter than λ_{adap}. This means that a change in α_2 needs to overcome this difference.

In figure 43 the left figure shows the results are included with the use of α_1 and α_2 of respectively 0.38 and 2.62 as derived earlier for the large original roughness ratio. A part of the results lies under the 10 percent deviation line, and after a closer look at the results these are the patterns with multiple patches. The parallel patterns are pretty good predicted. This indicates that the influence of the mixing width is good represented with a grid size of 20 m but that the influence of the adaptation of the flow behind the patches is underestimated, which means it is too rough predicted. This also makes sense because the influence of the less rough patch of trees is smaller than a patch of bushes. This will lead to a smaller adaptation length of the flow behind the patches, and this leads to a smaller increase in roughness by this adaptation of the flow. A decrease of α_2 is thus needed in order to increase the

prediction ability of the model. It turns out that a value of 1.7 for α_2 gives a better prediction of the aggregate Chézy values as can be seen in figure 34b.

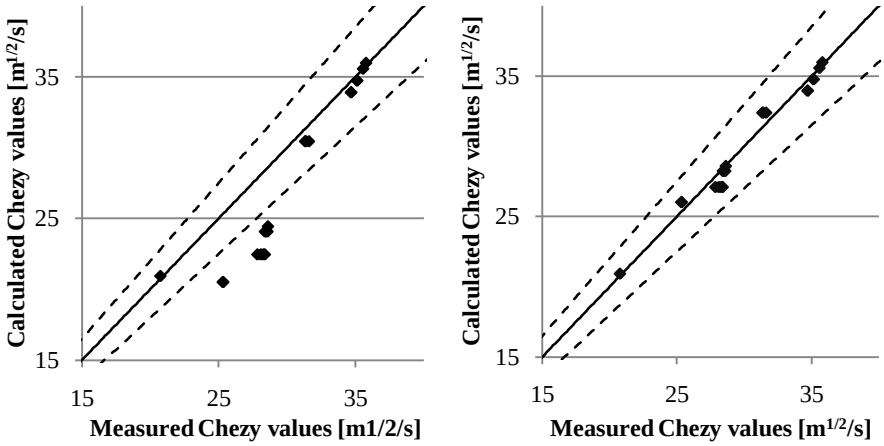

Figure 43: The calculated results plotted against the measured results for situations with a different roughness ratio. The solid line indicates perfect agreement and the dotted lines the 10 percent range. Left figure: α_2 of 2.62. Right figure: α_2 of 1.7.

To check whether this value is also accurate enough for situations that are not used to deduce the value, the patterns that are used in Van Velzen & Klaassen are also predicted and compared for situations with trees and grass. In figure 44 these results can be found. The black points are the results that are obtained with the use of the new model. All the values fall within the 10 percent deviation lines and are thus acceptable. The grey points are generated with the help of the WA-method. On average these lay further away from the perfect match line and in general the pattern does not follow this line. It can thus be concluded that also with these situations the new model gives a better prediction of the aggregate Chézy value than the now in use WA-method.

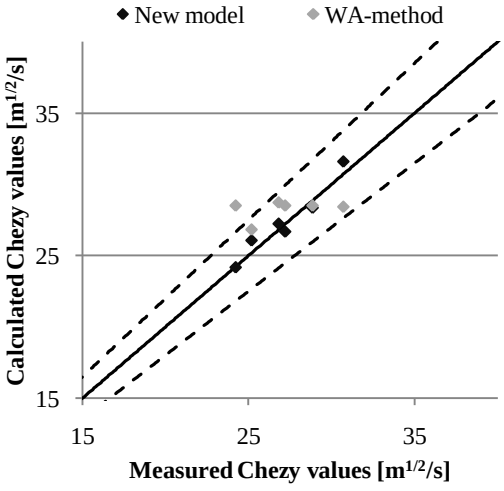

Figure 44: Comparison of the prediction capability of the new model (black dots) and the WA-method (grey dots) for patterns created by Van Velzen & Klaassen (1999) and a different roughness ratio. The solid line indicates perfect agreement and the dotted lines the 10 percent range.

6 DISCUSSION

In this chapter some elements of the research are critically reviewed. This is done in two separate parts; first the limitations of using a depth averaged flow model are discussed, and secondly the choices are discussed that were made in the used modeling situations and during the development of the new prediction method.

6.1 MODELING LIMITATIONS

A large series of model calculations using WAQUA are carried out in this study. The new prediction method is based on the results of these calculations. WAQUA is a depth averaged model and thus does not fully treat the flow processes in the water at a smooth-rough transition. Experiments with spatial variations in roughness (Vermaas, 2008) reveal that the secondary circulation induces an additional roughness. This effect is not taken into account in WAQUA. These influences are therefore not captured in the new prediction method. Assumptions are made based on the flow adaptation processes that are captured in WAQUA and thus might be incorrect compared to the more real situations. For example the assumption that the mixing layer width is constant along a rough patch can be considered wrong when the full three dimensional processes are included. This because in experiments a growth of the mixing layer along the rough area was observed (Van Prooijen, 2004).

Another discussion point, which is also related to the former point, is the implementation of the eddy viscosity coefficient. Because the model is depth averaged the turbulence effects cannot be modeled but need to be present; this is done by the eddy viscosity. But there is no real consensus in what value is the best for what situation. The help file of SIMONA and other papers give contradicting suitable eddy viscosity values. Because this value has a large influence on the mixing layer width, the choice of the eddy viscosity value influences the average accurateness of the new prediction model. With an increasing eddy viscosity value the accuracy decreases. It even turned out that in extreme situations with a high covering (larger than 70 percent) and a large eddy viscosity value the Chézy value predictions became unrealistic.

To understand the behaviour of the flow adjustment processes 3d models together with a turbulence model can be used to investigate these effects. The results of these runs can help in understanding the actual processes that take place and might help in adjusting the prediction method in such a way that the additional roughness due to the flow processes are better represented.

6.2 MODELING CHOICES AND ASSUMPTIONS

The large set of situations that is modeled in this study are all situations where the adaptation of the flow behind a patch cannot evolve fully. This leads to the implementation of the free space behind a patch as a parameter instead of the adaptation length that belongs to a certain patch size and water depth. For situations with a small part of the adaptation length present the new method can predict the aggregate roughness very accurate. Application of the new method in, for example, the one dimensional model SOBEK results in different situations than are used in this study. This because SOBEK uses large grid cells and thus a larger part of the flow adaptation can be present. Some assumptions that were made might not hold when the total flow adaptation can evolve. One assumption is that the average roughness value on the area that is influenced by flow adjustment

processes is the average Chézy value of the rough and the smooth vegetation type. This holds in situations with only a small part of the flow adaptation length. When the whole length is taken into account, this average Chézy value might be a wrong assumption. It is thought that not the average Chézy value should be taken as average roughness in the adaptation area, but a value more close to the roughness value belonging to the smooth vegetation type. This because the total length is very long compared to the length of the rough patch.

The only two vegetation types that are used in the investigation are bushes and grass. During the validation of the new method, situations with another roughness ratio, grass and trees, are predicted. The method however gives to rough predictions in these situations; especially the additional roughness due to the flow adaptation is too high. Because the ratio between the length of the free space behind a patch and the length of the rough patch is included this does not change with a varying roughness ratio. Changing the constant value (α_2) solved this problem. However this is not thought to be an accurate solution.

Some choices and assumptions that are made during the investigation give a limitation in applicability of the new method. Modeling more extreme situations can help to define applicability boundaries or improving the new method such that it is also usable in extreme situations.

Furthermore a complete serial pattern cannot be predicted very accurately by the new method. The serial function is capable of doing this in a very accurate manner but it is a drawback that the new prediction method cannot handle all the vegetation patterns that can be present on an area. This induces a more complex implementation in the method because two functions are needed. Taking the ratio between the total width of the area and the width of the rough vegetation area as boundary conditions when to use which method can solve this.

7 CONCLUSIONS AND RECOMMENDATIONS

This final chapter presents the conclusions of the study. This is done by answering the research questions provided in chapter 1 in order to achieve the objective of this study. Next several recommendations are given for future research. These recommendations are derived from the discussion in chapter 6 and the conclusions in paragraph 7.1.

7.1 ANSWERS TO RESEARCH QUESTIONS

The objective of this study was to get insight in what manner different parameters influence the way in which WAQUA measures the aggregate roughness over a vegetation pattern and to deduce a new prediction method that predicts the aggregate roughness value. In order to reach this objective four research questions were set up. The objective of this study is achieved by answering these questions.

> *How do we have to characterize the vegetation pattern in general parameters that control the aggregate roughness?*

In this study multiple situations with different pattern types were modeled with WAQUA in order to find out which parameters have an influence on the aggregate roughness. After investigation of the results it turns out that different parameter types are responsible for the aggregate roughness.

First of all the general direction to the flow, serial or parallel, has a large influence on the aggregate roughness. A serial oriented pattern will have an averagely larger roughness than a parallel oriented pattern. This can be explained by the amount of streamlining of the pattern. A parallel pattern has a large streamlining in the flow and a serial pattern a very low streamlining because in that situation all the water has to flow over the rough vegetation area. The pattern type with multiple square patches on the area has an average amount of streamlining in the flow.

Secondly the degree of covering of the rough vegetation has an influence on the aggregate roughness; the higher the degree of covering the higher the roughness. This covering itself can be expressed in dimensions of the rough patches and number of patches.

The areas of rough vegetation induce processes around the smooth-rough transitions: mixing layers along a rough patch and flow adaptation areas behind the patch. These processes are transition zones for the water to adapt to the flow conditions that belong to the new roughness situation.

The influences of the flow adaptation processes on the aggregate roughness are however influenced by the geometrical dimensions of the rough patches. The longer a patch the longer a mixing layer extends over the area and the wider a patch, the longer the adaptation of the flow is behind a patch. These two parameter types, geometrical and flow processes cannot be treated separately because the geometrical dimensions influence the flow processes. These processes also explain the large differences between a more serial or parallel oriented pattern (except a complete serial pattern). When the pattern is completely parallel only a mixing layer will have an influence on the aggregate roughness but when there is also smooth space behind the patches the adaptation of the flow will also have an influence.

This all together gives a set of parameters that are geometrical parameters, such as width and length of patches and lengths of free spaces and also flow process parameters such as the mixing layer and the adaptation of the flow behind the rough vegetation. These geometrical parameters influence the flow process parameters and vice versa.

How do the water depth and grid size have an influence on the aggregate roughness obtained with the model WAQUA on a floodplain with a pattern of two vegetation types?

The water depth has an influence on the aggregate roughness because the individual Chézy roughness values are influenced by the water depth. When the water depth is larger, relatively less water is influenced by the vegetation and thus the roughness will be lower. Because the Chézy value changes with water depth, the aggregate roughness due to the pattern is dependent by the water depth through the Chézy value.

Implementing a grid size of 10 or 20 m has no influence on the aggregate roughness. With a size of 10 m the calculation time and output is larger than with the 20 m case, thus implementing a grid size of 20 m can be preference because of this.

What is the deviation of the aggregate roughness value obtained from WAQUA model runs with different patterns of roughness patches compared with the WA-method?

The Chézy values obtained with WAQUA are generally overestimated by the WA-method. The larger the water depth the smaller the deviations, although the differences still range till 13 $m^{1/2}/s$ with a water depth of 7 m. With a water depth of 5 m, only 25.6 percent of the results fall within the 10 percent range around the measured Chézy values. Especially the parallel oriented patterns are poorly represented by the WA-method.

Can an improved roughness prediction method be developed instead of the WA-method by taking into account additional control parameters?

In chapter 5 a new method is developed that is better capable in predicting the aggregate roughness value than the WA-method. This method is based on the geometrical dimensions of the pattern and the flow processes that are induced by the smooth-rough vegetation transitions. The basis for the new method is the parallel function, which describes the roughness of a parallel pattern. The roughness induced by the mixing layer and the flow adaptation is assumed to be an additional roughness that needs to be subtracted from the parallel function. This additional roughness is made up of two contributions: i) the influence of the mixing layer, which is expressed as the ratio between the total mixing layer width and the width of the rough vegetation area, and ii) the ratio between the free space behind a rough patch and the length of the rough patch. If the adaptation length fits between patches then the adaptation length is used in terms of free space.

This new prediction method can give accurate predictions of the aggregate Chézy values. The measured Chézy values using model calculations with WAQUA are very well predicted by the new method. Almost all the predictions deviate less than 10 percent of the measured Chézy values.

The new method is also capable of predicting aggregate Chézy values in situations where the pattern lay out is irregular, which were not taken into account during the deviation of the prediction model. Situations with a different eddy viscosity were also validated. The eddy viscosity has an effect on the width of the mixing layer. The improved method can also give accurate Chézy value predictions in situations with different eddy viscosity coefficients. In situations where the roughness ratio between the smooth and rough vegetation is different, the new method needs a small modification.

7.2 RECOMMENDATIONS

Based on this research a few recommendations can be made. The first one relates to the manner in which the aggregate roughness of a vegetation pattern is obtained. This study is only based on the use of the model WAQUA. Because this is a depth averaged model some flow processes, such as turbulence, cannot be treated fully. Laboratory experiments can reveal in more detail the processes that take place around the smooth and rough transitions and this can help in understanding why certain patterns are more rough or smooth or even give an almost equal average roughness, while the pattern lay out is different.

The second recommendation relates to the relations that can describe the flow adaptation and the mixing layer width. In this study a relation was found between the water depth and width of the vegetation patch and the flow adaptation length. However a relation for the mixing layer width could not be found. Also the roughness ratio will have an influence on these flow adjustment processes but this ratio is not taken into account in this study. More generic relations can be deduced between the eddy viscosity coefficient, water depth and roughness ratio to calculate the mixing layer and the flow adaptation length that are generally applicable. These relations will increase the practical application of the new prediction method. With the help of more advanced 3d models together with turbulence model the mixing layer and the flow adaptation can more thoroughly be investigated. This will help in deriving a more generic relation for these processes.

The last recommendation is about the new method itself. It is proven in this study that it is possible to increase the accuracy of predicting the aggregate roughness when geometrical parameters of the pattern and flow characteristics resulting from these geometrical parameters are used. However it has not been tested whether it is possible to include this new prediction method in a model. Because the new prediction method needs more specific information of the vegetation pattern, the calculation time might increase. This is something that can be investigated in the future.

8 REFERENCES

Boderie, P., Icke, J., Kuijper, M., Meijers, E., Verspagen, J. & Juisman, J. (2005). Ontwikkeling 1- D Stofstromenmodel Noordelijk en Zuidelijk Deltabekken en 2-D Blauwalgenmodel Volkerak-Zoommeer. RIKZ.

Davis, J.C. (2002). Statistics and data analysis in geology (Third edition). United States of America: John Wiley & Sons, Inc.

Gao, Q. (2004). SOBEK-modellen voor het Markermeer en de Veluwerandmeren. RIZA werkdocument: 2004.191x

Labeur, R.J. (1998). Waterbeweging in zandwingebieden t.b.v. product K2000*Z.W.. Bureau Svašek, Rapport 98454/1081

Ministry of Transport, Public Works and Water Management (2008). User's guide WAQUA general information 10.51.

Ministry of Transport, Public Works and Water Management (2009a). User's guide WAQPRE. 10.97, October 2009.

Ministry of Transport, Public Works and Water Management (2009b). WAQUA/TRIWAQ two- and three-dimensional shallow water flows model. Technical documentation. SIMONA report number 99-01.

Praagman, N. (2005) Cursusboek gevorderden WAQUA in SIMONA. SIMONA rapportnr. 2005-05

Projectorganisatie Ruimte voor de Rivier. (2007) Planologische kernbeslissing ruimte voor de rivier. Nota van toelichting. Retrieved December 23, 2009 from http://www.ruimtevoorderivier.nl/Hoofdsite/menu/Meer%20info/Publicaties/PKB%20deel%204

Ribberink, J.S. & Hulscher, S.J.M.H. (2008). River dynamics. I: Shallow-water flows. Reader course 540040.

Rijkswaterstaat (2010a). Ecotopenatlas. Retrieved January 18, 2010 from http://www.rws.nl/water/natuur_en_milieu/ecotopen/ecotopenatlas/

Rijkswaterstaat (2010b). Ecotoop Rijntakken-Oost/Maas. Retrieved August 27, 2010 from: http://www.rijkswaterstaat.nl/images/2004%20-%202006%20Maas-midden%20west%20deelkaart4_tcm174-262657.pdf

RWS-Waterdienst & Deltares (2009a). Modelbeschrijving Maas Model. Versie: simona-maas-hr2006_4-v1.

RWS-Waterdienst & Deltares (2009b). Modelbeschrijving Rijn Model. Versie: simona-rijn-j95_4-v1.

Sieben, J. (2006). Ruwheidsformulering in waterbewegingsmodellen, verkenning. Werkdocument 2001.202x RIZA.

Straatsma, M.W. & Baptist, M.J. (2008). Floodplain roughness parameterization using airborne laser scanning and spectral remote sensing. Remote Sensing of Environment 112 (2008), 1062- 1080.

Svašek Hydraulics. (2010). WAQUA. Retrieved September 10, 2010 from http://www.svasek.com/modelling/waqua.htm

Uittenbogaard, R.E., Stolker, C., De Goede, E.D., Van Kester, J.A.Th.M., Jagers, H.R.A. & Wijbenga, J.H.A (2005). Eddy Viscositeit in WAQUA modellen van Rijntakken en Maas. Rijkswaterstaat, RIZA.

Van Prooijen, B.C. (2004). Shallow mixing layers. PhD thesis, TU Delft.

Van Velzen, E.H, & Klaassen, G. (1999). Verspreide en aaneengesloten gebieden met begroeiing. Studie naar het effect van begroeiingspatronen. Werkdocument 99.193x RIZA.

Van Velzen, E.H., Jesse, P., Cornelissen, P., & Coops, H. (2002). Stromingsweerstand vegetatie in uiterwaarden. Deel 2 achtergronddocument versie 1.0 RIZA werkdocument 2002.141x.

Van Velzen, E.H., Jesse, P., Cornelissen, P. & Coops, H. (2003). Stromingsweerstand vegetatie in uiterwaarden. Deel 1 handboek versie 1-2003. RIZA rapport 2003.028.

Vermaas, D.A. (2008). Mixing layers in open channel flow with abrupt bed roughness changes. Master Thesis.

Vreugdenhil, C.B. (1994). Numerical methods for shallow-water flow. Dordrecht, Kluwer Academic Publishers.

Vollebregt, E.A.H., Roest, M.R.T & Lander, J.W.M. (2002). Large scale computing at Rijkswaterstaat. Parallel Computing Volume 28, Issue 1 January 2003, p 1-20.

Zong, L. & Nepf, H. (2010). Flow and depostition in and around a finite patch of vegetation. Geomorphology 116 (2010) 363-372.

9 APPENDICES

I RESISTANCE FORMULATIONS AS DEDUCED IN VAN VELZEN & KLAASSEN (1999)

a. Formulation parallel flow:

$$C_t = \sum_i x_i C_{ri}$$

b. Formulation for spread vegetation: In this formulation the area of flow of for example parcels of natural trees or bushes thinned out over the total area.

$$C_t = \frac{1}{\sqrt{\frac{C_d \cdot A_v \cdot x/100 \cdot h}{2g} + \frac{1}{C_0^2}}}$$

c. Formulation for one group of vegetation (adapted formula of Klaassen (according to Van Velzen & Klaassen (1999)).

$$C_t = \sqrt{\frac{C_g^2}{1-\lambda+\alpha\cdot\beta\cdot\frac{B}{L}(1-\frac{\gamma}{1-\beta(1-\gamma)})(c-1+1/3(c-1)^2)+\lambda c^2}}$$

$$\beta = \frac{b}{B}$$

$$\lambda = \frac{l}{L}$$

$$\gamma = \frac{C_b}{C_g}$$

$$c = \frac{1}{1+\beta(\gamma-1)}$$

$$b' = \frac{\gamma\beta}{(\beta-1)+\gamma}\cdot b$$

With:

C_g	= Chézy value of grass	[$m^{1/2}/s$]
C_b	= Chézy value of trees	[$m^{1/2}/s$]
C_t	= Chézy value for the combination	[$m^{1/2}/s$]

x	= Coverage percentage	[%]
A_v	= Average area vegetation of flow	[m^2]
C_d	= Drag coefficient	[-]
h	= Water depth	[m]
C_0	= Chézy coefficient under grow	[$m^{1/2}/s$]
g	= Acceleration of gravity	[m/s^2]
i	= slope	[-]
B	= Total width floodplain	[m]
L	= Total length floodplain	[m]
b	= Width area with trees	[m]
l	= Length area with trees	[m]
α	= Measure for the adaptation length	[m]

The derivation of these formula's can be found in Van Velzen & Klaassen (1999).

II (OLD) VEGETATION PATTERNS

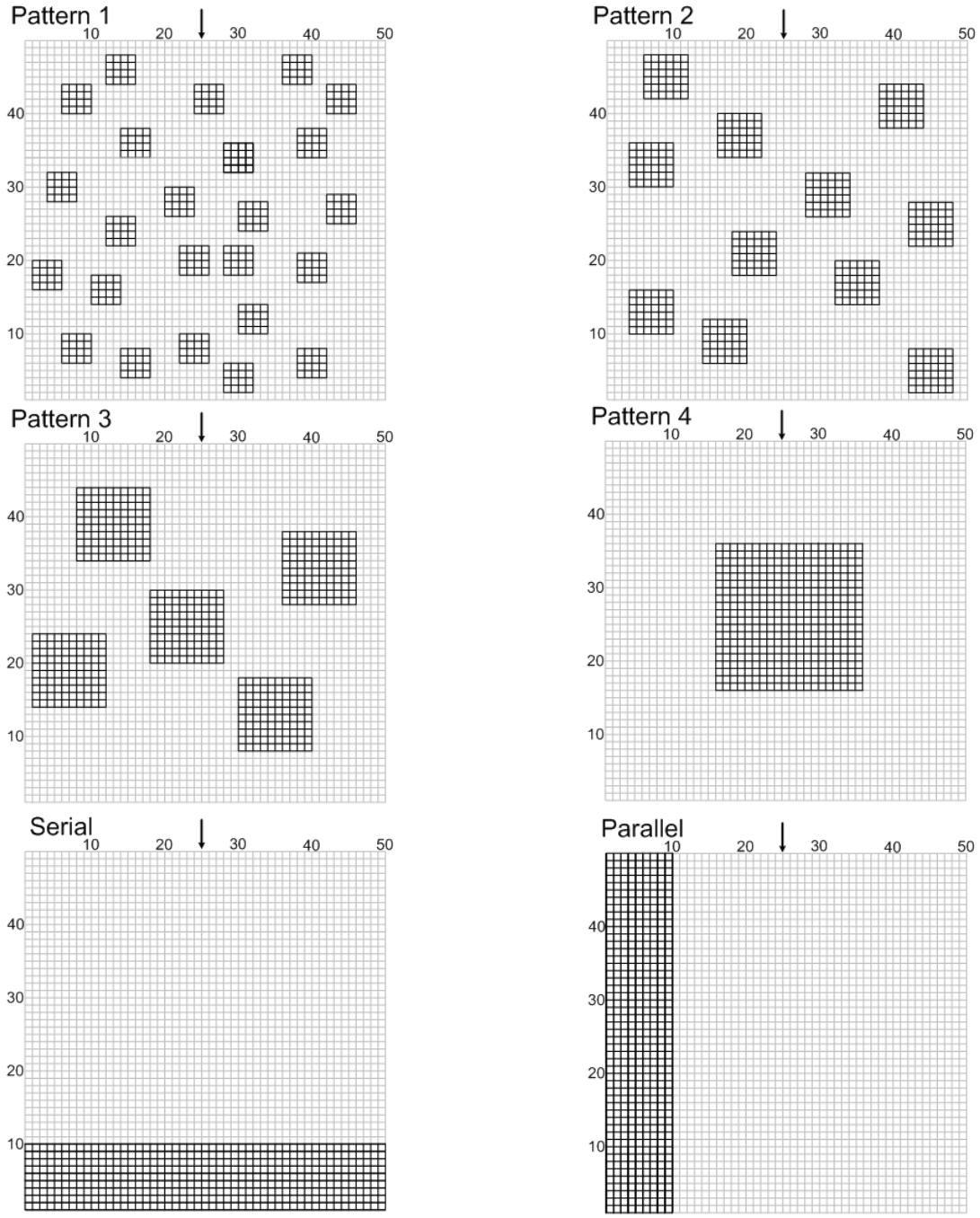

Figure 45: Left top: 24 randomly placed plots with 16% coverage, left middle: 5 randomly placed plots with 20.8% coverage, left bottom: one stripe perpendicular to the flow direction with 20% covering. Right top: 11 randomly placed plots with 16.5% covering, right middle: one plot with 16.7% coverage, right bottom: one stripe parallel to the flow direction with 18.75% coverage (Van Velzen & Klaassen, 1999)

III PLOTS WITH WEIGHTING METHODS

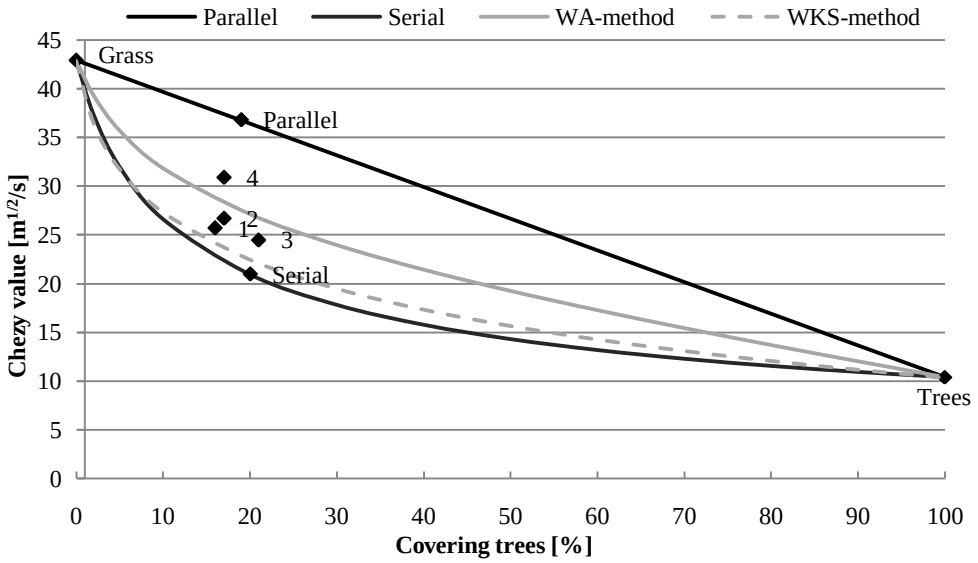

Figure 46: Influence pattern trees on the Chézy value (Van Velzen and Klaassen, 1999)

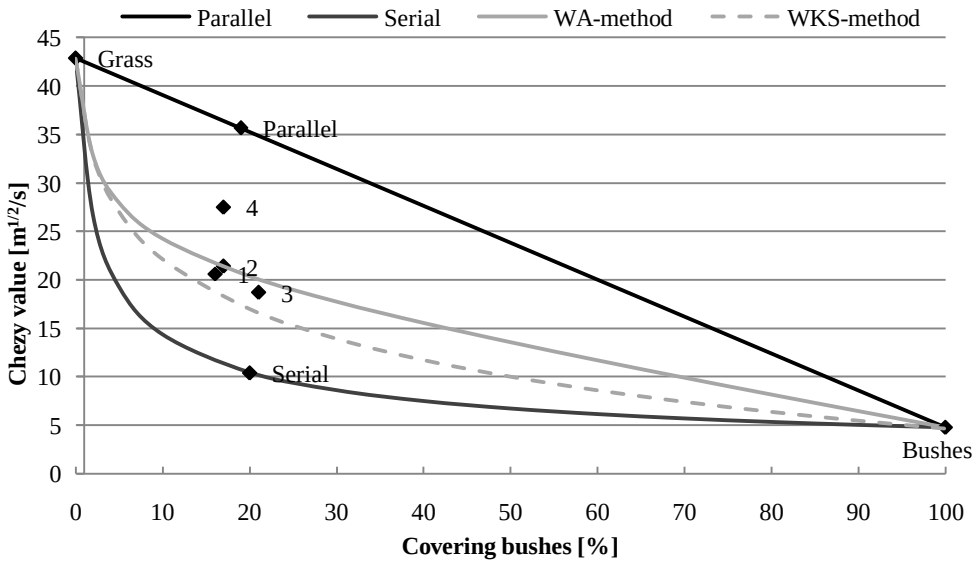

Figure 47: Influence pattern bushes on the Chézy value (Van Velzen and Klaassen, 1999)

IV DERIVATION PARALLEL AND SERIAL FORMULAS

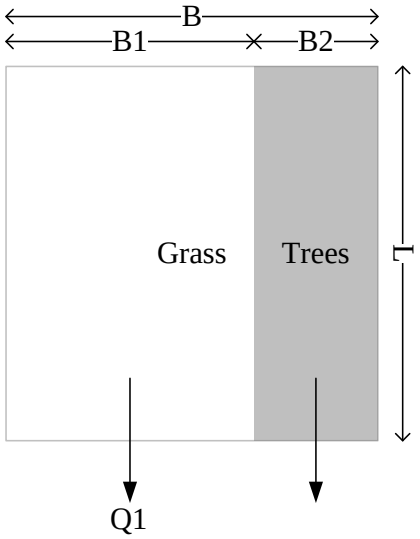

Figure 48: Concept of parallel flow

For parallel flow the formula can be deduced in the following manner:

$$Q_1 = h \cdot B_1 \cdot C_g \cdot \sqrt{hi}$$

$$Q_2 = h \cdot B_2 \cdot C_w \cdot \sqrt{hi}$$

$$Q_t = h \cdot B \cdot C_t \cdot \sqrt{hi}$$

$$Q_t = Q_1 + Q_2$$

Everything filled in gives:

$$h \cdot B \cdot C_t \cdot \sqrt{hi} = h \cdot B_1 \cdot C_g \cdot \sqrt{hi} + h \cdot B_2 \cdot C_w \cdot \sqrt{hi}$$

$$B \cdot C_t = B_1 \cdot C_g + B_2 \cdot C_w$$

Expressing this in the coverage of trees: $x = \frac{B_2}{B}$ gives:

$$C_t = (1 - x)C_g + xC_w \rightarrow \underline{C_t = \sum_i x_i C_i}$$

For serial flow:

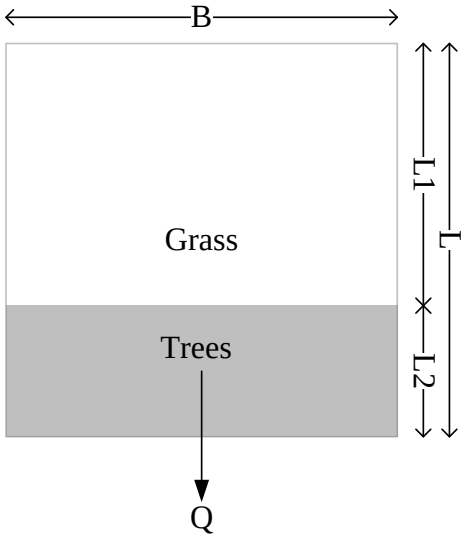

Figure 49: Concept of serial flow

$$Q_t = Q_1 = Q_2$$

$$Q_1 = h \cdot B \cdot C_g \cdot \sqrt{hi_1}$$

$$Q_2 = h \cdot B \cdot C_w \cdot \sqrt{hi_2}$$

$$Q_t = h \cdot B \cdot C_t \cdot \sqrt{h\frac{(i_1 \cdot L_1 + i_2 \cdot L_2)}{L}}$$

After inserting the expression of i_1 and i_2 gives:

$$C_t = \frac{1}{\sqrt{\frac{\frac{B_1}{C_g^2} + \frac{B_2}{C_w^2}}{L}}}$$

Expressing this in the coverage of wood $x = \frac{B_2}{B}$ gives:

$$C_t = \frac{1}{\sqrt{\frac{1-x}{C_g^2} + \frac{x}{C_w^2}}} \rightarrow \frac{1}{\sqrt{\sum_i \frac{x_i}{C_i^2}}}$$

V OUTLAY OF THE PARALLEL PATTERNS

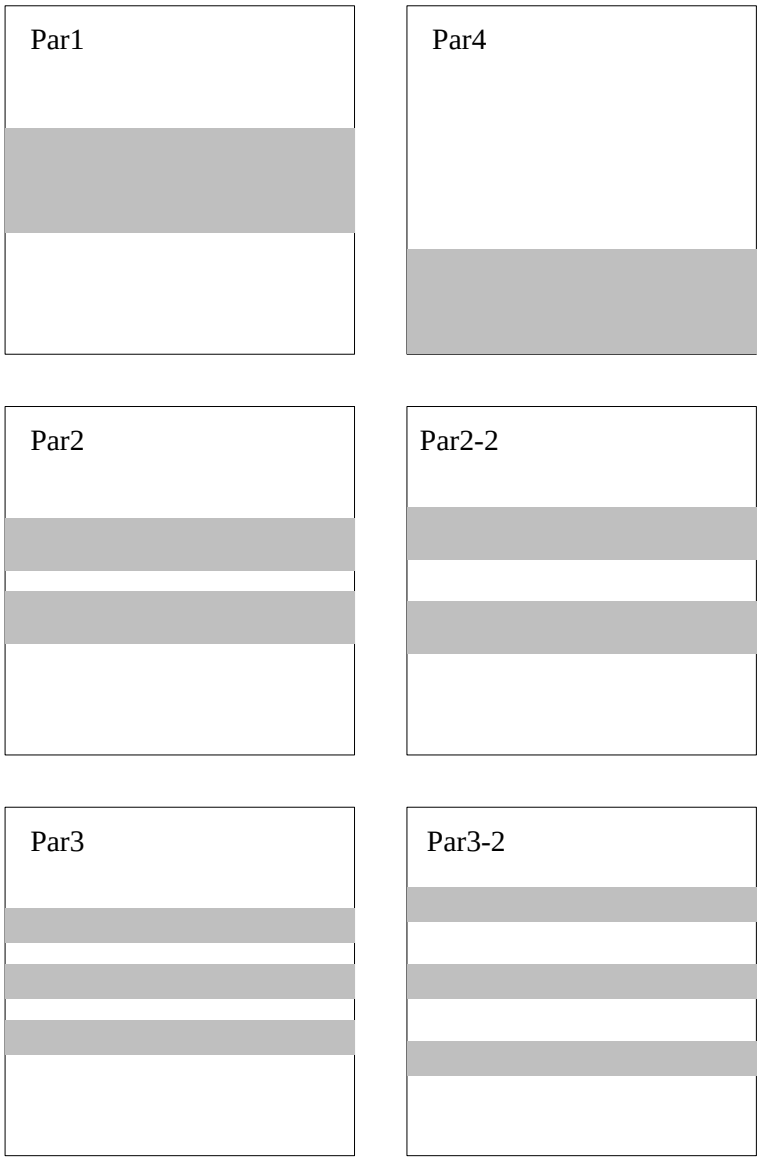

Figure 50: Lay out of the parallel patterns.

VI MODEL RESULTS

VI-A WATER DEPTH 5 M GRID SIZE 20 M

Covering		Parallel patterns					Pattern with two patches				
	Pattern type	1	2	2-2	3	3-2	4	21	22	23	24	25	26
10%	Discharge [m^3/s]	4252	4184	4183	4117	4115	4287	3107	3110	3835	3792	3731	3719
	Chézy [$m^{1/2}/s$]	38.0	37.4	37.4	36.8	36.8	38.3	27.8	27.8	34.3	33.9	33.4	33.3
20%	Discharge [m^3/s]	3830	3761	3760	3692	3691	3865	2165	2155	3295	3263	3256	-
	Chézy [$m^{1/2}/s$]	34.3	33.6	33.6	33.0	33.0	34.6	19.4	19.3	29.5	29.2	29.1	-
30%	Discharge [m^3/s]	3407	3338	3337	3269	3268	3442	1543	1538	2915	2931	-	-
	Chézy [$m^{1/2}/s$]	30.5	29.9	29.9	29.2	29.2	30.8	13.8	13.8	26.1	26.2	-	-
40%	Discharge [m^3/s]	2984	2915	2915	2847	2845	3019	-	-	-	-	-	-
	Chézy [$m^{1/2}/s$]	26.7	26.1	26.1	25.5	25.4	27.0	-	-	-	-	-	-
70%	Discharge [m^3/s]	1716	1647	1647	1578	1612	1751	-	-	-	-	-	-
	Chézy [$m^{1/2}/s$]	15.3	14.7	14.7	14.1	14.4	15.7	-	-	-	-	-	-

Covering		Pattern with four patches				Pattern with nine patches				Serial
	Pattern type	41	42	43	44	91	92	93	94	
10%	Discharge [m^3/s]	3472	3476	3427	3427	3418	3422	3327	3317	1568
	Chézy [$m^{1/2}/s$]	31.1	31.1	30.6	30.7	30.6	30.6	29.8	29.7	14.0
20%	Discharge [m^3/s]	2784	2773	2761	2742	2723	2694	2674	2624	1141
	Chézy [$m^{1/2}/s$]	24.9	24.8	24.7	24.5	24.4	24.1	23.9	23.5	10.2
30%	Discharge [m^3/s]	2290	2262	2263	2232	2198	2172	2158	2113	941
	Chézy [$m^{1/2}/s$]	20.5	20.2	20.2	20.0	19.7	19.4	19.3	18.9	8.4
40%	Discharge [m^3/s]	1901	1874	1885	1854	1817	1776	1805	1757	820
	Chézy [$m^{1/2}/s$]	17.0	16.8	16.9	16.6	16.3	15.9	16.1	15.7	7.3
70%	Discharge [m^3/s]	1014	1018	1014	1019	-	-	-	-	623
	Chézy [$m^{1/2}/s$]	9.1	9.1	9.1	9.1	-	-	-	-	5.6

VI-B WATER DEPTH 5 M GRID SIZE 10 M

Covering		Parallel patterns					Pattern with two patches					
	Pattern type	1	2	2-2	3	3-2	4	21	22	23	24	25	26
10%	Discharge [m^3/s]	4251	4161	4160	4070	4068	4297	3084	3093	3849	3820	3764	3764
	Chézy [$m^{1/2}/s$]	38.0	37.2	37.2	36.4	36.4	38.4	27.6	27.7	34.4	34.2	33.7	33.7
20%	Discharge [m^3/s]	3826	3736	3735	3645	3786	3872	2146	2133	3311	3297	3289	-
	Chézy [$m^{1/2}/s$]	34.2	33.4	33.4	32.6	33.9	34.6	19.2	19.1	29.6	29.5	29.4	-
30%	Discharge [m^3/s]	3402	3311	3310	3221	3219	3447	1520	1514	2990	2974	-	-
	Chézy [$m^{1/2}/s$]	30.4	29.6	29.6	28.8	28.8	30.8	13.6	13.5	26.7	26.6	-	-
40%	Discharge [m^3/s]	2977	2886	2886	2798	2794	3023	-	-	-	-	-	-
	Chézy [$m^{1/2}/s$]	26.6	25.8	25.8	25.0	25.0	27.0	-	-	-	-	-	-
70%	Discharge [m^3/s]	1703	1612	1611	1522	1523	1748	-	-	-	-	-	-
	Chézy [$m^{1/2}/s$]	15.2	14.4	14.4	13.6	13.6	15.6	-	-	-	-	-	-

Covering		Pattern with four patches				Pattern with nine patches				Serial
	Pattern type	41	42	43	44	91	92	93	94	
10%	Discharge [m^3/s]	3463	3469	3431	3430	3398	3404	3310	3297	1569
	Chézy [$m^{1/2}/s$]	31.0	31.0	30.7	30.7	30.4	30.5	29.6	29.5	14.0
20%	Discharge [m^3/s]	2800	2786	2770	2748	2689	2656	2638	2583	1141
	Chézy [$m^{1/2}/s$]	25.0	24.9	24.8	24.6	24.0	23.8	23.6	23.1	10.2
30%	Discharge [m^3/s]	2273	2207	2255	2224	2198	2157	2173	2114	941
	Chézy [$m^{1/2}/s$]	20.3	19.7	20.2	19.9	19.7	19.3	19.4	18.9	8.4
40%	Discharge [m^3/s]	1888	1860	1879	1847	1784	1751	1781	1733	819
	Chézy [$m^{1/2}/s$]	16.9	16.6	16.8	16.5	16.0	15.7	15.9	15.5	7.3
70%	Discharge [m^3/s]	1008	1018	1026	1039	-	-	-	-	623
	Chézy [$m^{1/2}/s$]	9.0	9.1	9.2	9.3	-	-	-	-	5.6

VI-C WATER DEPTH 3 M, GRID SIZE 20 M

Covering		Parallel patterns						Pattern with two patches					
	Pattern type	1	2	2-2	3	3-2	4	21	22	23	24	25	26
10%	Discharge [m^3/s]	1776	1749	1749	1721	1721	1790	1349	1356	1634	1621	1604	1591
	Chézy [$m^{1/2}/s$]	34.2	33.7	33.7	33.1	33.1	34.4	26.0	26.1	31.4	31.2	30.9	30.6
20%	Discharge [m^3/s]	1579	1552	1552	1525	1525	1593	891	889	1404	1370	1355	-
	Chézy [$m^{1/2}/s$]	30.4	29.9	29.9	29.3	29.3	30.7	17.1	17.1	27.0	26.4	26.1	-
30%	Discharge [m^3/s]	1383	1356	1356	1328	1328	1397	583	581	1203	1204	-	-
	Chézy [$m^{1/2}/s$]	26.6	26.1	26.1	25.6	25.6	26.9	11.2	11.2	23.1	23.2	-	-
40%	Discharge [m^3/s]	1187	1159	1159	1132	1132	1200	-	-	-	-	-	-
	Chézy [$m^{1/2}/s$]	22.8	22.3	22.3	21.8	21.8	23.1	-	-	-	-	-	-
70%	Discharge [m^3/s]	597	570	570	542	556	611	-	-	-	-	-	-
	Chézy [$m^{1/2}/s$]	11.5	11.0	11.0	10.4	10.7	11.8	-	-	-	-	-	-

Covering		Pattern with four patches				Pattern with nine patches				Serial
	Pattern type	41	42	43	44	91	92	93	94	
10%	Discharge [m^3/s]	1484	1484	1464	1466	1449	1456	1410	1413	112
	Chézy [$m^{1/2}/s$]	28.6	28.6	28.2	28.2	27.9	28.0	27.1	27.2	2.2
20%	Discharge [m^3/s]	1187	1184	1174	1170	1137	1131	1118	1104	79
	Chézy [$m^{1/2}/s$]	22.8	22.8	22.6	22.5	21.9	21.8	21.5	21.2	1.5
30%	Discharge [m^3/s]	973	967	955	950	936	932	891	880	65
	Chézy [$m^{1/2}/s$]	18.7	18.6	18.4	18.3	18.0	17.9	17.1	16.9	1.3
40%	Discharge [m^3/s]	789	782	759	752	745	732	702	691	57
	Chézy [$m^{1/2}/s$]	15.2	15.0	14.6	14.5	14.3	14.1	13.5	13.3	1.1
70%	Discharge [m^3/s]	309	309	309	291	-	-	-	-	43
	Chézy [$m^{1/2}/s$]	5.9	5.9	5.9	5.6	-	-	-	-	0.8

VI-D WATER DEPTH 7 M, GRID SIZE 20 M

Covering		Parallel patterns					Pattern with two patches					
	Pattern type	1	2	2-2	3	3-2	4	21	22	23	24	25	26
10%	Discharge [m^3/s]	7514	7390	7387	7270	7266	7578	5374	5364	6517	6483	6455	6516
	Chézy [$m^{1/2}/s$]	40.6	39.9	39.9	39.3	39.2	40.9	29.0	29.0	35.2	35.0	34.9	35.2
20%	Discharge [m^3/s]	6814	6689	6687	6564	6559	6878	3939	3917	5669	5649	5697	-
	Chézy [$m^{1/2}/s$]	36.8	36.1	36.1	35.4	35.4	37.1	21.3	21.1	30.6	30.5	30.8	-
30%	Discharge [m^3/s]	6114	5989	5986	5864	5859	6178	3045	3038	5081	5145	-	-
	Chézy [$m^{1/2}/s$]	33.0	32.3	32.3	31.7	31.6	33.4	16.4	16.4	27.4	27.8	-	-
40%	Discharge [m^3/s]	2984	2915	2915	2847	2845	3019	-	-	-	-	-	-
	Chézy [$m^{1/2}/s$]	26.7	26.1	26.1	25.5	25.4	27.0	-	-	-	-	-	-
70%	Discharge [m^3/s]	3313	3188	3186	3061	3122	3377	-	-	-	-	-	-
	Chézy [$m^{1/2}/s$]	17.9	17.2	17.2	16.5	16.9	18.2	-	-	-	-	-	-

Covering		Pattern with four patches				Pattern with nine patches				Serial
	Pattern type	41	42	43	44	91	92	93	94	
10%	Discharge [m^3/s]	5885	5887	5846	5842	5899	5903	5811	5783	3844
	Chézy [$m^{1/2}/s$]	31.8	31.8	31.6	31.5	31.9	31.9	31.4	31.2	20.8
20%	Discharge [m^3/s]	4791	4763	4793	4751	4749	4693	4727	4630	2876
	Chézy [$m^{1/2}/s$]	25.9	25.7	25.9	25.7	25.6	25.3	25.5	25.0	15.5
30%	Discharge [m^3/s]	4006	3954	3991	3933	3931	3880	3902	3819	2397
	Chézy [$m^{1/2}/s$]	21.6	21.3	21.5	21.2	21.2	20.9	21.1	20.6	12.9
40%	Discharge [m^3/s]	3419	3369	3410	3356	3324	3258	3333	3245	2098
	Chézy [$m^{1/2}/s$]	18.5	18.2	18.4	18.1	17.9	17.6	18.0	17.5	11.3
70%	Discharge [m^3/s]	2096	2102	2096	2105	-	-	-	-	1608
	Chézy [$m^{1/2}/s$]	11.3	11.4	11.3	11.4	-	-	-	-	8.7

VII PREDICTION NEW METHOD FOR 3 AND 7 M WATER DEPTH

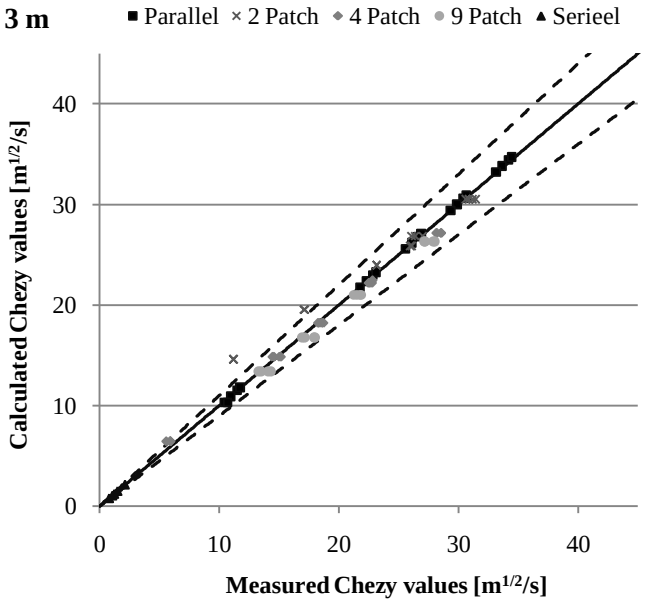

Figure 51: Calculated Chézy values plotted against the measured Chézy values of all the patterns with a water depth of 3m. The solid line indicates perfect agreement and the dotted lines the 10 percent range.

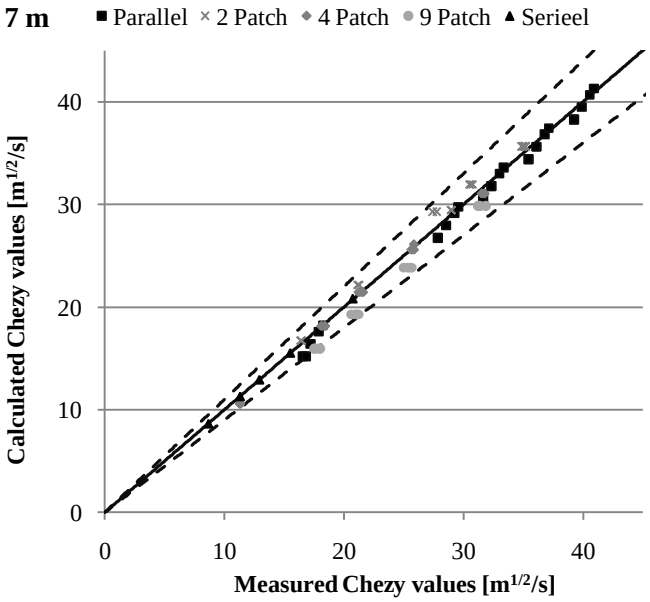

Figure 52: Calculated Chézy values plotted against the measured Chézy values of all the patterns with a water depth of 7m. The solid line indicates perfect agreement and the dotted lines the 10 percent range.